(2)

NAVAL POSTGRADUATE SCHOOL
Monterey, California

THESIS

RADIATION SIGNATURES FROM AN EXTERNAL RELATIVISTIC ELECTRON BEAM

by

Wee, Kyoum Bok
December 1988

Thesis Advisor : Xavier K. Maruyama

Approved for public release; distribution is unlimited

SECURITY CLASSIFICATION OF THIS PAGE

REPORT DOCUMENTATION PAGE

1a. REPORT SECURITY CLASSIFICATION: Unclassified	1b RESTRICTIVE MARKINGS
2a. SECURITY CLASSIFICATION AUTHORITY	3. DISTRIBUTION/AVAILABILITY OF REPORT: Approved for public release; distribution is unlimited
2b. DECLASSIFICATION/DOWNGRADING SCHEDULE	
4. PERFORMING ORGANIZATION REPORT NUMBER(S)	5. MONITORING ORGANIZATION REPORT NUMBER(S)
6a. NAME OF PERFORMING ORGANIZATION: Naval Postgraduate School; 6b. OFFICE SYMBOL (If applicable): 61	7a. NAME OF MONITORING ORGANIZATION: Naval Postgraduate School
6c. ADDRESS (City, State, and ZIP Code): Monterey, California 93943-5000	7b. ADDRESS (City, State, and ZIP Code): Monterey, California 93943-5000
8a. NAME OF FUNDING/SPONSORING ORGANIZATION; 8b. OFFICE SYMBOL (If applicable)	9. PROCUREMENT INSTRUMENT IDENTIFICATION NUMBER
8c. ADDRESS (City, State, and ZIP Code)	10. SOURCE OF FUNDING NUMBERS: PROGRAM ELEMENT NO. / PROJECT NO. / TASK NO. / WORK UNIT ACCESSION NO.

11. TITLE (Include Security Classification)

RADIATION SIGNATURES FROM AN EXTERNAL RELATIVISTIC ELECTRON BEAM

12. PERSONAL AUTHOR(S) Wee, Kyoum Bok

13a. TYPE OF REPORT	13b TIME COVERED	14. DATE OF REPORT (Year, Month, Day)	15. PAGE COUNT
Master's Thesis	FROM _____ TO _____	1988 December	69

16. SUPPLEMENTARY NOTATION The views expressed in this thesis are those of the author and do not reflect the official policy or position of the Department of Defense or the U.S. Government.

17. COSATI CODES		
FIELD	GROUP	SUB-GROUP

18. SUBJECT TERMS (Continue on reverse if necessary and identify by block number)

Cerenkov radiation, Transition radiation, Normalization, has been observed, Theses, LLNL

19. ABSTRACT (Continue on reverse if necessary and identify by block number)

We have observed x-band radiation which occurs when an electron beam travelling in air traverses an aluminum plate. The radiation pattern is more complicated than can be explained with a simplified model of Cerenkov radiation from air and transition radiation from the aluminum-air interface. The empirical observation is that the peak angle decreases with energy until about 70 MeV, then increases with energy. The angular width of the peak distribution shows a similar behavior with energy. The observed peak angle decreases as the distance from the horn antenna to the aluminum foil is increased. The explanation of the radiation distribution observed is not yet satisfactory. A major improvement in the data accumulation process has been inteoduced by measuring radiation at a fixed angle as data is taken with a movable horn. This procedure allows us to compensate for the fluctuating electron beam intensity. The data can now be digitized and stored in a computer for analysis. Previous experiments allowed only for analog measurements. Further work, both theoretical and experimental, will be required to understand fully the radiation signature of the electron beam. Keywords:)

20. DISTRIBUTION/AVAILABILITY OF ABSTRACT: ☒ UNCLASSIFIED/UNLIMITED ☐ SAME AS RPT. ☐ DTIC USERS	21. ABSTRACT SECURITY CLASSIFICATION: Unclassified
22a. NAME OF RESPONSIBLE INDIVIDUAL: Professor Xavier K. Maruyama	22b. TELEPHONE (Include Area Code): (408) 646-2431; 22c. OFFICE SYMBOL: 61Mx

DD FORM 1473, 84 MAR 83 APR edition may be used until exhausted. All other editions are obsolete

SECURITY CLASSIFICATION OF THIS PAGE

Approved for public release; distribution is unlimited.

Radiation Signatures from an External
Relativistic Electron Beam

by

Wee, Kyoum Bok
Major, Republic of Korea Army
B.S., Republic of Korea Military Academy, 1978

Submitted in partial fulfillment of the
requirements for the degree of

MASTER OF SCIENCE IN PHYSICS

from the

NAVAL POSTGRADUATE SCHOOL
December 1988

Author: Kyoum B. Wee
Wee, Kyoum Bok

Approved by: Xavier K. Maruyama
Xavier K. Maruyama, Thesis Advisor

Fred R Bushick
Fred R. Bushick, Second Reader

Karlheinz E. Woehler, Chairman,
Department of Physics

Gordon E. Schacher,
Dean of Science and Engineering

ABSTRACT

We have observed x–band radiation which occurs when an electron beam travelling in air traverses an aluminum plate. The radiation pattern is more complicated than can be explained with a simplified model of Cerenkov radiation from air and transition radiation from the aluminum–air interface. The empirical observation is that the peak angle decreases with energy until about 70 MeV, then increases with energy. The angular width of the peak distribution shows a similar behavior with energy. The observed peak angle decreases as the distance from the horn antenna to the aluminum foil is increased. The explanation of the radiation distribution observed is not yet satisfactory.

A major improvement in the data accumulation process has been introduced by measuring radiation at a fixed angle as data is taken with a movable horn. This procedure allows us to compensate for the fluctuating electron beam intensity. The data can now be digitized and stored in a computer for analysis. Previous experiments allowed only for analog measurements.

Further work, both theoretical and experimental, will be required to understand fully the radiation signature of the electron beam.

TABLE OF CONTENTS

I. INTRODUCTION 1

A. PREVIOUS EXPERIMENTS AT THE NPS LINAC 1

B. PURPOSE 2

C. BACKGROUND 2

II. THE EXPERIMENT 14

A. EXPERIMENTAL SETUP 14

B. PROCEDURE 18

III. RESULTS AND DISCUSSIONS 21

A. RESULTS 21

B. DISCUSSIONS 35

1. Comparison of Theoretical Angle and Experimental Angle 35

2. Measured Angle and Adjusted Angle 37

3. Normalization of the Observed Radiation Intensity 39

4. Peak Angle versus Electron Energy 39

5. Peak Angle versus Distance between Foil and Antenna 43

6. Width of the Intensity Lobes 45

IV. CONCLUSIONS 50

APPENDIX A: OPERATING CHARACTERISTICS OF NPS LINAC 51

APPENDIX B: PROGRAM FOR THE NORMALIZED INTENSITY and RAW DATA 52

LIST OF REFERENCES 57

INITIAL DISTRIBUTION LIST 58

LIST OF FIGURES

1. Cerenkov Radiation 4

2. Transition Radiation Produced in the Forward Direction at An Interface 8

3. Diffraction Transition Radiation of Wave Vector **k** Produced by a Particle of Velocity **v** Transiting a Distance R from the Center of a Hole 11

4. Schematic Diagram of Experimental Setup 15

5. Schematic Diagram of the Radiation Measurement Arrangement 16

6. Feedhorn Assembly 17

7. Schematic Geometry of Measurement at 77 inches Distance 19

8. The Normalized Intensity of Observed Radiation vs. Angle. The Electron Energy is 45 MeV and the Distance is 77 Inches 23

9. The Normalized Intensity of Observed Radiation vs. Angle. The Electron Energy is 45 MeV and the Distance is 58 Inches 24

10. The Normalized Intensity of Observed Radiation vs. Angle. The Electron Energy is 45 MeV and the Distance is 48 Inches 25

11. The Normalized Intensity of Observed Radiation vs. Angle. The Electron Energy is 45 MeV and the Distance is 38 Inches 26

12. The Normalized Intensity of Observed Radiation vs. Angle. The Electron Energy is 65 MeV and the Distance is 77 Inches 27

13. The Normalized Intensity of Observed Radiation vs. Angle. The Electron Energy is 65 MeV and the Distance is 58 Inches 28

14. The Normalized Intensity of Observed Radiation vs. Angle. The Electron Energy is 65 MeV and the Distance is 48 Inches 29

15. The Normalized Intensity of Observed Radiation vs. Angle. The Electron Energy is 65 MeV and the Distance is 38 Inches 30

16. The Normalized Intensity of Observed Radiation vs. Angle. The Electron Energy is 80 MeV and the Distance is 77 Inches 31

17. The Normalized Intensity of Observed Radiation vs. Angle. The Electron Energy is 80 MeV and the Distance is 58 Inches 32

18. The Normalized Intensity of Observed Radiation vs. Angle. The Electron Energy is 80 MeV and the Distance is 48 Inches 33

19. The Normalized Intensity of Observed Radiation vs. Angle. The Electron Energy is 80 MeV and the Distance is 38 Inches 34

20. Theoretical Angle and Experimental Angle vs. Electron Energy 36

21. Normalization with Bad Raw Data 40

22. Normalization with Good Raw Data 41

23. Peak Angle versus Electron Energy 42

24. Peak Angle versus Distance 44

25. Definition of FWHM 47

26. FWHM versus Energy 48

27. Experimental Station 51

ACKNOWLEDGEMENTS

I wish to express my gratitude and appreciation to Professor Xavier K. Maruyama and Professor Fred R. Buskirk for the instruction, guidance and advices throughout this research.

Also, assistance of Mr. D. Snyder and Mr. H. M. Rietdyk for the operation and maintenance of the NPSLinac is greatly appreciated.

Finally, many thanks to my wife, Ji–Young and my son, Dong–Yoon, for their love and being healthy and patient for two and half years in Monterey, California.

This paper is dedicated to my boy Dong–Yoon.

I. INTRODUCTION

A. PREVIOUS EXPERIMENTS AT THE NPS LINAC

The study of the radiation signatures from a relativistic electron beam external to the accelerator and beam transport system has been the subject of many studies at the Naval Postgraduate School electron linear accelerator. There were many efforts to measure microwave Cerenkov radiation from an electron beam traversing through air. In 1982, Saglam did an experiment showing that microwave radiation could be observed at angles larger than expected from the classical Cerenkov radiation angle of 1.3 degrees [Ref. 1]. This radiation was interpreted as Cerenkov radiation which showed diffraction effects due to finite interaction length effects. This result was confirmed by Bruce in 1985 [Ref. 2].

As the electron beam passes from the linac into the air through a kapton vacuum – air interface, transition radiation (TR) can also occur. In 1986, O'Grady did an experiment to observe that radiation [Ref. 3]. In addition, if the beam travels through an aperture, the radiation generated is diffraction radiation (DTR). TR is a special case of DTR where the aperture size becomes vanishingly small. Lee attempted to measure DTR in 1987, but found that the radiation observed could not neatly be classified as Cerenkov, transition or diffraction radiation [Ref. 4].

The experiment presented here is a continuation of the efforts to understand the full nature of the radiation signature which is produced when an electron beam travelling in a dielectric medium (air), passes through a conductor (Al). Although our original hope was to measure diffraction transition radiation, because of the

difficulty in understanding our measurement results, we have left that experiment to later effort. We have, instead, concentrated our efforts to distinguishing between TR and Cerenkov radiation and have not considered DTR. The interpretation of the observed radiation is still inconclusive, but it is hoped that this work will contribute to future efforts. We suspect that the interpretation is being impeded because the signature we are observing include Cerenkov radiation, transition radiation, their interference, and the effects of a finite interaction length.

B. PURPOSE

This experiment is primarily focused to distinguish the angular dependence of the Cerenkov and TR according to different energy and distance. We also investigate the distribution of radiation intensity as a function of distance and the beam energy. A third focus is to improve the analyzed method of recording data. Previous work [Ref. 4] at NPS linac. assumed the beam density to be stable; however, the beam is unstable and sometimes goes to zero. Because the radiation field is dependent on the beam intensity, the observed raw data should be corrected to consider changes in the beam intensity. We call the radiation intensity corrected for the fluctuation beam intensity, the normalized intensity.

C. BACKGROUND

1. HISTORY

Cerenkov radiation is commonly seen as the pale blue or bluish–white light emitted from a transparent medium that surrounds a source of high radioactivity. The pale blue light was observed by Mme. Curie in 1910 with bottles of concentrated radium solutions. The first experimental work on the phenomenon

was reported in 1926 by L. Mallet and then in 1934 by P. A. Cerenkov, who performed a complete set of experiments dealing with this phenomenon until 1938. In 1937 a classical explanation for the radiation was proposed by I. M. Frank and I. Tamm. Cerenkov's experiments were in excellent agreement with the theory of Frank and Tamm. In 1940 V. L. Ginzburg advanced a quantum theory for the radiation. From then on it was known as Cerenkov radiation. In 1958, J. V. Jelley wrote a text on Cerenkov radiation covering theory through current research [Ref. 5]. Cerenkov radiation is useful in research because from observations of it, charged particles can be detected and their speeds measured.

In the original theory put forth by Frank and Tamm [Ref. 5], they assumed an infinite medium and constant velocity. In actuality both the medium traversed and the length of the particle's path are finite. The finite path introduces diffraction effects, and the boundaries of the medium changes the total radiation yield, adding a contribution known as transition radiation to the Cerenkov radiation. Because both Cerenkov and transition radiation have the same polarization, it is difficult to separate the two effects.

Another form of radiation can be introduced considering charged particles entering a hole in a screen or approaching near a screen. The radiation produced is known as diffraction transition radiation or diffraction radiation [Ref. 6]. This was discovered much more recently and is associated with transition radiation. The theory describing diffraction radiation caused by a beam of bunched charged particles is still quite tentative, with little experimental verification. It appears that one method available to distinguish between Cerenkov, transition and diffraction transition radiation will be through an analysis of changes generated in the angular dependence of the diffraction pattern.

2. Brief Theory of Cerenkov Radiation

Cerenkov radiation results when a charged particle moves through a transparent medium (e.g., air, water, glass, etc.) at a velocity that is greater than the velocity of light c', in the medium. The charged particle causes the medium along its track to be momentarily polarized and generates a short electromagnetic pulse to each elemental region of the medium along the track. The fields then propagate to large distances,as radiation, but only if v is grater than c' [Ref. 5]. The radiation propagates at the Cerenkov angle, $\cos \Theta_c = \frac{c'}{v}$, where $c' = c/n$ and n is the refractive index of the medium and c is the speed of light in vacuum.

Coherence of the radiation occurs only at the angle θ_c. The radiation fields move a shorter distance (c't) during a time increment of t than does the particle (vt) as shown in Figure 1. This relative movement has been likened to the

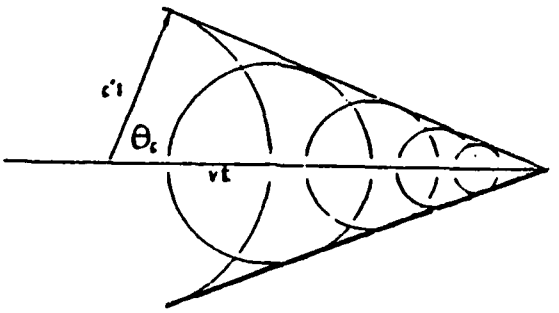

Idealized Cerenkov radiation in a medium with a high n

Figure 1. Cerenkov radiation

wake of a ship or the shock wave generated by an object in air travelling faster than the speed of sound. Jelley uses the Huygen's principle to explain the wave front coherence [Ref. 5]. This assumes that the radiation is observed at infinity and that the particle's path is infinite in length. In reality, however, all media are dispersive, and absorption bands exist throughout the spectrum, bringing the radiation to finite levels [Ref. 5]. Since Cerenkov radiation occurs in three dimensions, the wave front takes the shape of a cone as in Figure 1 (Figure 2.3, [Ref. 5]).

If the interaction length is finite compared to the wavelength, then the radiation power is dependent on the observation angle described by a diffraction pattern. See equation (1). The power of Cerenkov radiation from periodic electron bunches, such as in an linac, in a medium of finite interaction length was calculated by Buskirk and Neighbours [Ref. 7], in work accomplished at NPS in 1982. Expanding their study a year later, Neighbours and Buskirk calculated the diffraction effects in Cerenkov radiation [Ref. 8]. This work resulted in the following relation in watts/steradian

$$W(\nu,\hat{n}) = \nu_o^2 Q R^2 \ \text{(watts/steradian)} \qquad (1)$$

where $Q = \frac{uc}{8\pi} q^2$

q = charge in electron bunch

ν_o= frequency of the linac (2.86 GHz)

$R = kL \sin\theta\, I(u)\, F(\vec{k})$

and where

$k = \frac{2\pi}{\lambda}$: wave number of Cerenkov radiation

$= jk_o$: j = integer, k_o = wave number for ν_o

L = finite interaction beam length

I(u) = sin(u)/u : diffraction pattern,

$u = \frac{kL(\cos\theta_c - \cos\theta)}{2}$

θ = observation angle from the beam direction

$F(\vec{k})$ = form factor of the charge distribution bunch.

The significance of equation (1) is that the radiated power depends upon the angle θ, measured to the beam in accordance with the diffraction pattern function, I(u). The form factor, $F(\vec{k})$, will be considered unity because the bunch length of the electron beam is small compared to the observed radiation wavelength. We must consider the distance to the far field for finite interaction length in the third harmonics. The operating characteristics of the NPS electron linear accelerator are contained in Appendix A.

3. Brief Theory of Transition Radiation

Transition radiation occurs when a charged particle of constant speed passes through a boundary where the properties of the medium change. Often the boundary is between two different dielectric media, but a dielectric–conductor, dielectric vacuum, or conductor–vacuum interface suffices to produce transition radiation. If the two media have different optical properties, then a charged particle will always produce transition radiation which will be dependent on the trajectory of the particle and the angle of particular interest. When a charged particle travelling through a solid, gas or plasma encounters a density change, it will also produce transition radiation [Ref. 9]. Although closely associated with Cerenkov radiation, the properties of transition radiation are quite different. The intensity is strongly dependent on the energy of the charged particle causing the generated spectrum to

extend from the microwave to x–ray region, where the upper limit is proportional to the Lorentz factor, γ, ($\gamma = 1 / \sqrt{1-\beta^2}$). Consider a charged particle crossing a single interface from medium I to medium II with dielectric permittivity ϵ_1 and ϵ_2 respectively, see Figure 2, (Figure 2, [Ref. 9]). In crossing this single interface, it is assumed that the path of the particle is normal to the interface. Ginsburg and Frank developed the following equation which is the transition radiation intensity observed in medium II [Ref. 10]

$$\frac{dI_2(\hat{n},\omega)}{d\omega\, d\Omega} = \frac{e^2v^2\sqrt{\epsilon_2}\ \sin^2\theta_2\cos^2\theta_2}{\pi^2\ c^3} * \left| \frac{(\epsilon_1-\epsilon_2)(1-\beta^2\epsilon_2-\beta\sqrt{\epsilon_1-\epsilon_2\sin^2\theta_2})}{(1-\beta^2\epsilon_2\cos^2\theta_2)(1-\beta\sqrt{\epsilon_1-\epsilon_2\sin^2\theta_2})(\epsilon_1\cos\theta_2+\sqrt{\epsilon_1\epsilon_2-\epsilon_2^2\sin^2\theta_2})} \right|^2 \qquad (2)$$

In Equation (2) $d\Omega$ is a solid angle about θ_2, the angle of observation measured from normal to the surface, $\beta = v/c$ with c the velocity of light in a vacuum. The TR intensity per unit frequency observed in medium I, $\frac{dI_1(\hat{n},\ \omega)}{d\omega\, d\Omega}$, can be obtained from above equation by interchanging subscripts 1 and 2 and letting $\beta \rightarrow -\beta$. The unit vector $\hat{n}$ is in the direction of propagation of the radiation being observed. In medium I, θ_1 is measured from the normal vector pointing into medium I, i.e., along $-\vec{v}$. Consider a particle going from a medium to a vacuum, then $\epsilon_2 = 1$. In addition if $\beta \cong 1$ and $|\epsilon_1| >> 1$ as for a metal, then Equation (2) is reduced to

$$\frac{dI_1}{d\omega\, d\Omega} = \frac{e^2\beta^2}{\pi^2 c} \frac{\sin^2\theta_1}{(1-\beta^2\cos^2\theta_1)^2} \qquad (3)$$

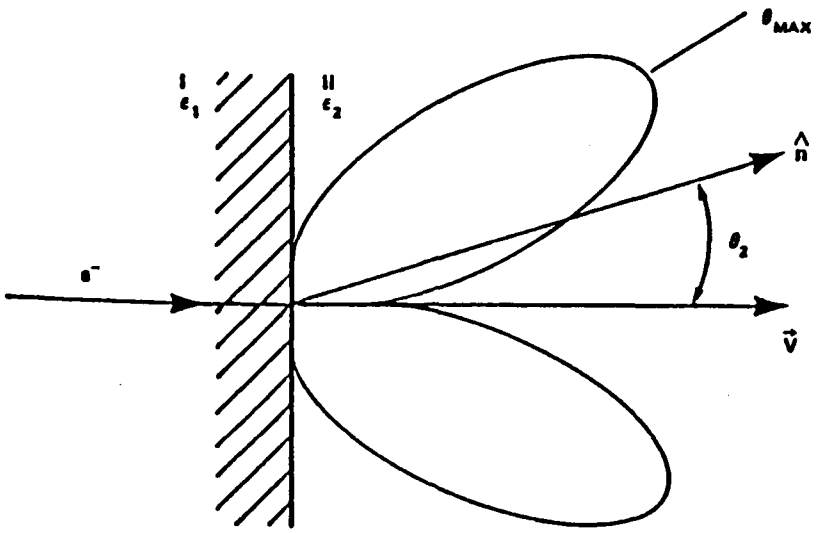

Notes : Medium I and medium II have dielectric functions ϵ_1 and ϵ_2. The direction of observation is n at an angle θ_2 with respect to the particle velocity v. Not shown is the backward TR which has similar intensity

Figure 2. Transition radiation produced in the forward direction at an interface

If the particle goes from vacuum to medium, $\epsilon_1 = 1$ and we obtain

$$\frac{dI_1}{d\omega\, d\Omega} = \frac{e^2\beta^2}{\pi^2 c} \frac{\sin^2\theta_1}{(1-\beta^2\cos^2\theta_1)^2} \left| \frac{\sqrt{\epsilon_2} - 1}{\sqrt{\epsilon_2} + 1} \right|^2 \tag{4}$$

which has the form of Equation (3) times the Fresnel reflection formula for light normally incident on a medium.

Transition radiation is polarized so that the electric vector lies in the plane containing $\hat{n}$ and the normal to the interface (or the particle velocity $\vec{v}$) and angularly dependent. For relativistic particles normally incident to the interface, the maximum intensity occurs at the angle [Ref. 9]

$$\theta_p = 1/\gamma = mc^2/E \tag{5}$$

where E is the total energy and mc^2 is the rest energy of the particle and γ is the Lorentz factor. It is this property which differs significantly from that of Cerenkov radiation where the dependence is primarily on the particle velocity.

4. Brief Theory of Diffraction Transition Radiation

Diffraction transition radiation, a phenomenon closely associated with transition radiation, is produced by a charged particle of constant velocity passing through a hole or near any interface between two media which possess different dielectric constants. This radiation is known to occur in linear accelerators when bunched charges lose energy in transiting the radio frequency accelerating modules This is known as "beam loading" [Ref. 9].

Although much research has been done on diffraction transition radiation, it pertains to a single charged particle. The physical aspect of diffraction transition radiation involves fast particles of constant velocity, the Huygens principle and scattering of virtual–photons. In this discussion, the field of the fast particle is considered equal to a set of plane waves. Ter–Mikaelian considers the fast particle passing through a circular hole [Ref. 6]. The calculation of the diffraction problem is similar to a procedure for calculating the diffraction of light waves, as well as involving scattering based on the Huygens principle. This method is valid if the wavelength, λ, incident on the hole is small compared to the radius of the hole. Additionally, deflection angles of the incident wave direction must be small (that is, only small deviations from the laws of geometrical optics can be tolerated). This should satisfy the following two conditions: the wavelength is much smaller than the hole radius and the angle of the produced radiation relative to the beam is much smaller than 1. These two conditions should be maintained provided the radiation process is viewed as scattering of virtual–photons. Using the Huygens principle to calculate the radiation introduces peculiarities because the charged particle field depends on the distance along the path. Ter–Mikaelian concludes that diffraction radiation of frequency, ω, will occur if the wavelength divided by the hole radius is greater than or approximately equal to the inverse of Lorentz factor ($\frac{\lambda}{a} \geq \gamma^{-1}$). The better this condition is fulfilled the greater will be the intensity of the diffraction radiation. Consider a charged particle, which has velocity v, passes through a hole of radius a using the condition with R representing an off distance as in Figure 3 (Figure 10, [Ref. 9]).

$$\frac{\gamma v}{\omega} >> a \text{ and } R << a \qquad (6)$$

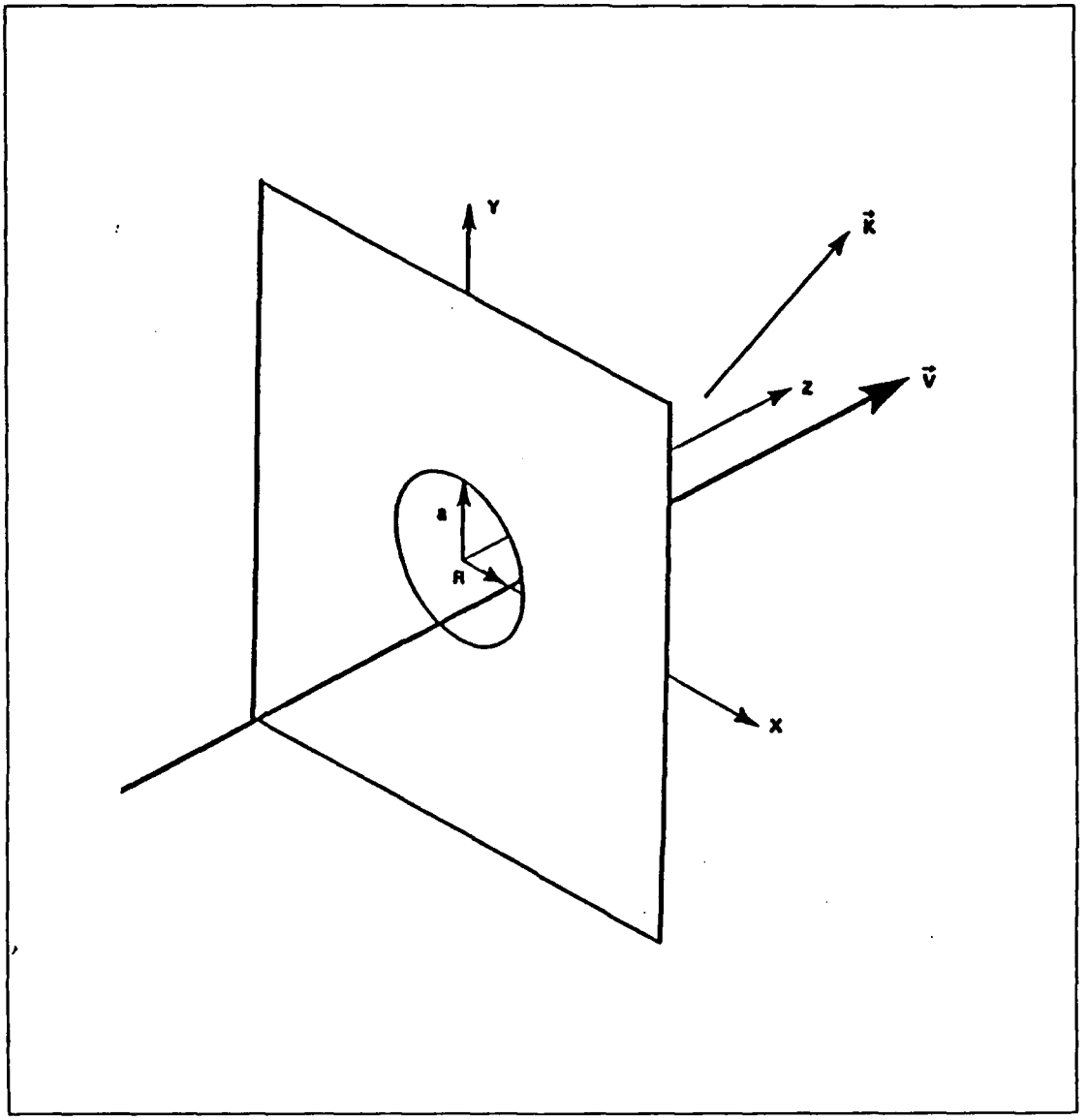

Figure 3. Diffraction transition radiation of wave vector $\vec{k}$ produced by a particle of velocity v transiting a distance R from the center of a hole of radius a in a screen

Ter–Mikaelian developed an expression for the number of quanta of frequency ω radiated in the range $d\theta$ about the observation angle θ by one electron which is (Equation (31.15), [Ref. 9])

$$N d\omega d\theta = \frac{1}{137\pi} \frac{\theta^3 d\theta}{(\gamma^{-2}+\theta^2)^2} [J_o^2(qa) + (\frac{R}{a})^2 J_1(qa)] \frac{d\omega}{\omega} \qquad (7)$$

where the factor q in the argument of the Bessel functions $J_o(qa)$ and $J_1(qa)$ is the projection of the wave vector $\vec{k}$ into the plane z=0 of Figure 3, i.e., $q = k\sin\theta$, and the angle of $\vec{q}$ with respect to the x–axis is ψ [Ref. 9:p. 28]. If R = 0 and Equation (6) is satisfied, the electric field components are

$$E_x = \frac{ie}{2\pi^2 c} \frac{q}{q^2 + \alpha^2} J_o(qa) \cos\psi \qquad (8)$$

$$E_y = \frac{ie}{2\pi^2 c} \frac{q}{q^2 + \alpha^2} J_o(qa) \sin\psi \qquad (9)$$

where $\alpha = \omega/(\gamma v)$. From the Equation (8) and (9) it is seen that the radiation is polarized with the electric vector lying in the plane containing $\vec{k}$ and $\vec{v}$. The θ–dependence of diffraction radiation is characteristic of that for transition radiation except for the hole in the screen which causes the Bessel functions to arise. Rule and Fiorito state that coherent diffraction radiation should be produced if the separation of the bunches in the particle beam are on the order of or smaller than the wavelength. Diffraction radiation will be produced by a beam at wavelength satisfying the relation

$$n_b^{-1/3} \leq \lambda \qquad (10)$$

where n_b is the beam electron density. The more this relation is satisfied the more that both transition and diffraction radiation will be enhanced and the intensity of radiation will become proportional to n_b^2. This coherent behavior has applications in beam diagnostics.

II. THE EXPERIMENT

A. EXPERIMENTAL SETUP

The experimental arrangement of this experiment is basically identical to that used by Lee [Ref. 4]. Figure 4 schematically represents the experimental setup. Figure 5 outlines the radiation measurement arrangement. In the experimental station is situated the feed horn assembly, a beam monitor, an aluminum plate and two research amplifiers. The electron beam bunches come from the linac through a beam pipe which may generate diffraction transition radiation (DTR), and through a plastic KAPTON aperture which may produce transition radiation (TR). On the end of the beam pipe, the beam goes through air where Cerenkov radiation is generated, then enters aluminum foil which may produce transition radiation. The beam may also generate Cerenkov radiation in the air after traversing the aluminum foil.

The feedhorn assembly, Figure 6, consists of an x–band microwave horn antenna, a short piece of x–band waveguide, and a mounting assembly holding the feedhorn which allows the feedhorn to rotate through an angle to measure the angular dependence of the reflected radiation. The center of the horn antenna, which receives radiated beam from aluminum foil, is located along the axis of the beam and maintained at the same vertical level while rotating from side to side by a travelling dolly. The speed of the travelling dolly is controlled by a variable speed control in the control room. The microwave signal is transmitted to the research amplifier through RG 9/U coaxial cable. A relatively weak signal is amplified with

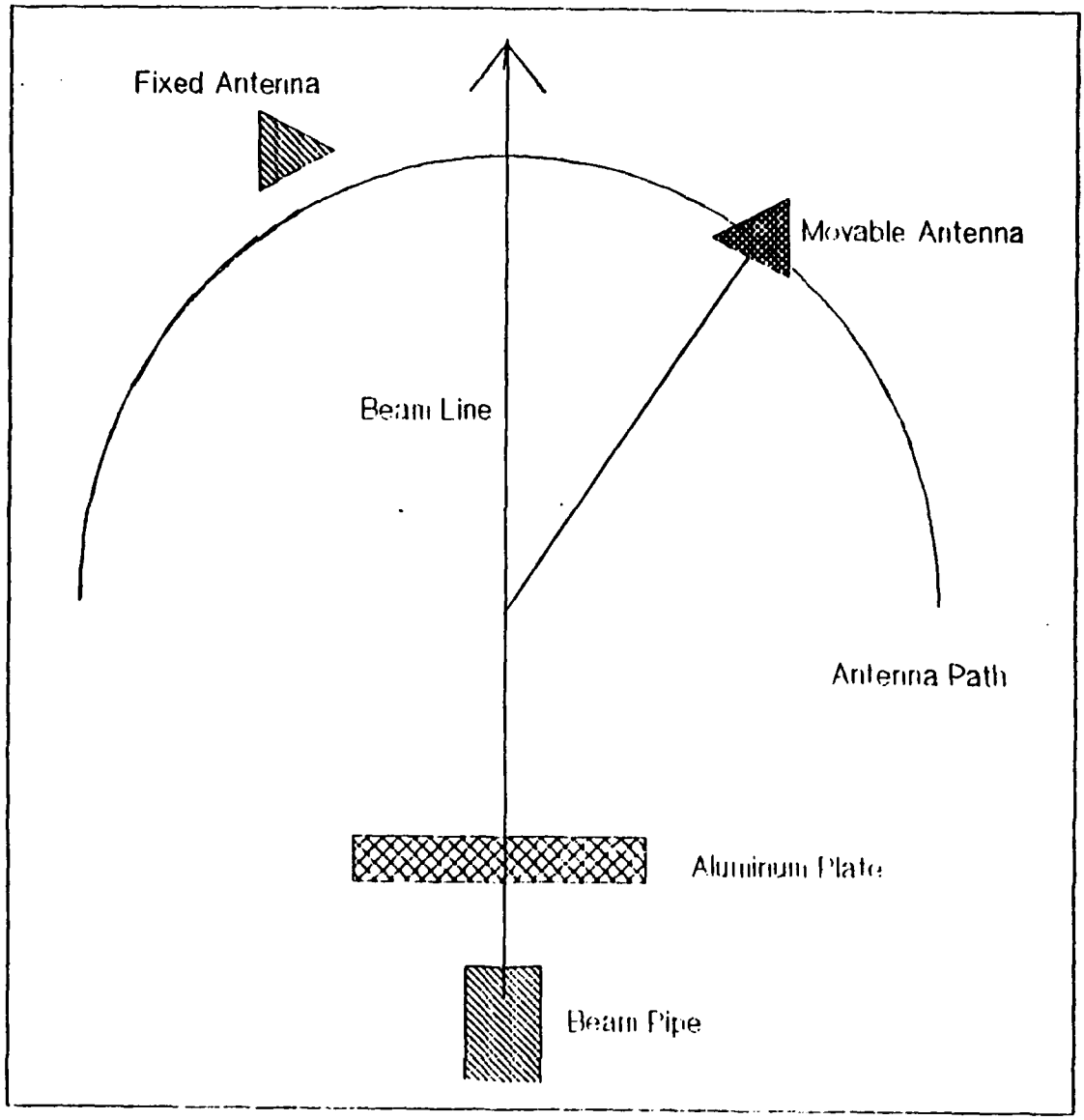

Figure 4. Schematic Diagram of Experimental Setup

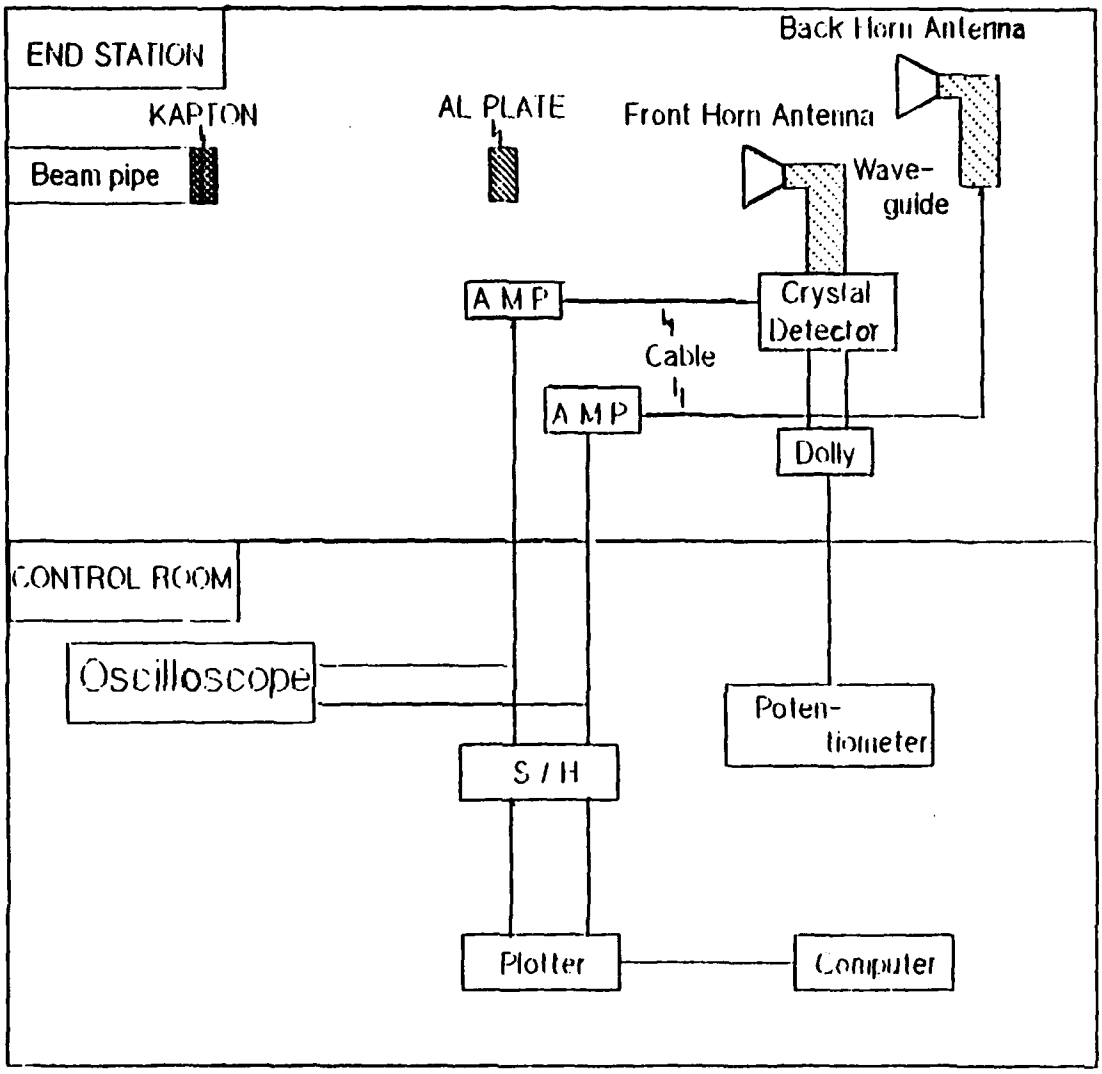

Figure 5. Schematic Diagram of the Radiation Measurement Arrangement

Figure 6. Feedhorn Assembly

two amplifiers with maximum 3000 gain. One measures the beam intensity, the other measures the raw data for the TR signal as the horn travels in the arc. These amplified signals are transmitted to the control room by triply shielded cable.

Upon entering the control room, a signal splitter is used to divert the signal into an oscilloscope for visual reference and to the data collection network. The data collection network is composed of a sample and hold network, an oscilloscope, a plotter, and a computer. Sample and hold circuit is the device which store analog information and reduce the aperture time of an analog–to–digital (A/D) converter. It is simply a voltage–memory device in which an input voltage is acquired, sample mode, and then stored on a high quality capacitor which is hold mode. Another oscilloscope is used for integration timing for the sample and hold network. After this network, signals are transmitted to the programmable HP7090A plotter through two channels, one to observe the beam intensity and the other to record the raw data. The plotter can take one thousand digitized data per each channel during a given period and plot the data itself or be controlled by a computer. An HP236 computer was used to control the plotter and save the raw data and provided a program written in basic language (see Appendix 2).

B. PROCEDURE

This experiment can be divided into three steps which are collection, normalization, and digitization of the signals. Until now, most experimental data at NPS was obtained by manually recording values from the oscilloscope or from the spectrum analyzer at angles observed through the closed circuit television. Great improvement was done by Bruce [Ref. 2] using the X/Y recorder in which the data was recorded automatically. However, all data was analog in form and no

manipulation of data was possible because of its analog nature.

Lee solved this problem by using a HP7090A plotter [Ref. 4]. Three channels are available for receiving analog input signals and each channel uses its own analog–to–digital (A/D) converter to digitize the analog input. It has three buffers that are used to store digitized input signal data during buffered recording and each buffer is capable of storing 1000 data values in a given period. The period for acquisition of the signal can be set from 1 sec to 24 hours. We can use this buffered data for drawing or for transferring to the computer. Also, it can plot the modified data from a computer. That is, the plotter serves as the front end of a data acquisition system or as a graphics plotter with a computer.

The second step is normalization of the raw data. Since the radiation field is dependent on the beam intensity the observed raw data should be corrected when the beam changes. This correction is called normalization. If the beam is constant, the signal should be stable when the detector is fixed. The observed raw data is divided by the beam intensity to obtain the normalized radiation intensity.

The last step of this experiment is digitization. In HP7090A plotter, there are three channels which are available for receiving analog input signals and each channel uses its own A/D converter to digitize the analog input. We can see the digitized data, which is converted from analog input, by using HP236 computer program (see Appendix 2). Since radiations are produced by a beam bunch moving at a constant velocity and a boundary (KAPTON, aluminum plate) is perpendicular to the electron beam, the electric field of the radiations will be in the plane of the beam direction and the detector. The magnetic field will be perpendicular to this plane. Therefore, it is expected all radiations appear together.

Even though radiation is observed, we don't know exactly what is TR, DTR, and Cerenkov radiation because we are unable to isolate the radiation according to each theory. So, we think there is a certain radiation including TR, DTR, and Cerenkov radiation when we operate the machine because TR and DTR are naturally produced from the end of the beam pipe, and Cerenkov radiation is generated in air.

We operate machine inserting a material between beam exit and the circumference of the wooden arm using different electron energies and different distances from the beam exit, analyzed the angular dependence of the results and compared to the theory of TR and Cerenkov radiation. We can use any material if the index of refractive of the material is greater than 1. This time we used thin aluminum foil which has 1.0024 for an index of refraction [Ref. 11]. At the first time, we put the material 77 inches from the arc of lever arm and later decreased the distance to 58 inches, 48 inches and 38 inches.

III. RESULTS AND DISCUSSIONS

A. RESULTS

Five different energies (30 Mev, 45 Mev, 65 Mev, 80 Mev, 90 Mev) and four different distances (77 inches, 58 inches, 48 inches, 38 inches) were used in this experiment. Refer to Figure 7.

The peak angle of T.R. should get smaller when the energy increases and the peak angle of Cerenkov radiation should get bigger with increasing the speed of the charged particle. However, for relativistic electrons the speed changes very slightly with increasing energy. An analysis of the functional dependence in the angular distribution of the diffraction pattern may be able to distinguish among Cerenkov, transition and diffraction radiation. All radiations are associated with a beam bunch moving at a constant velocity. Also, if the boundary (KAPTON window or Al plate) is perpendicular to the electron beam, then all radiations will have the electric field in the plane of the beam vector and observer, and the magnetic field will be perpendicular to the plane of the beam vector and observer. Data are shown in Figure 8 through Figure 19. Figure 8 through Figure 11 were obtained with electrons of 45 MeV energy. Figure 12 through Figure 15 were obtained with electrons of 65 MeV energy and Figure 16 through Figure 19 were obtained with electrons of 80 MeV energy. Normalized intensities can be compared between figures as the amplifier gains were kept constant. Each figure represents a minimum of three runs on the plotter travelling in both directions to obtain reproducible data. The results of this experiment will be broken down into three categories: (1) Comparison of observed peak angle versus electron energy, (2) Comparison of

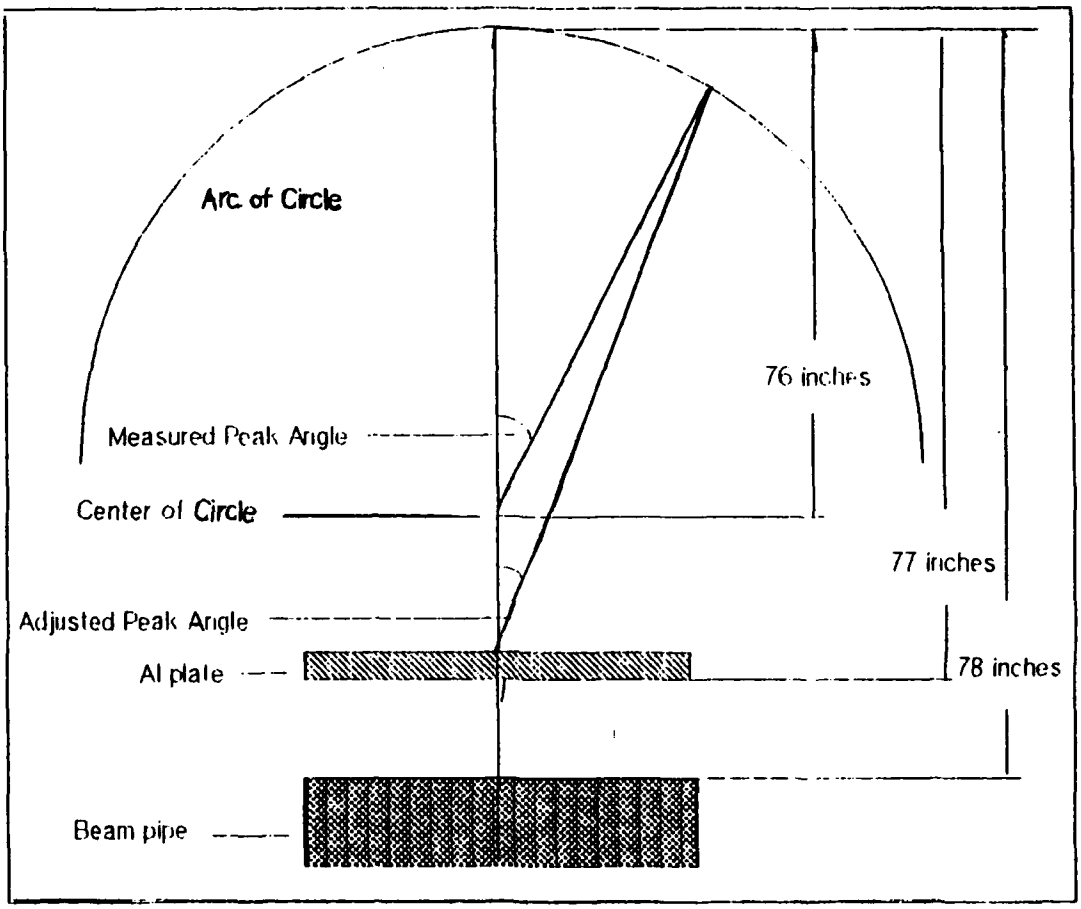

Figure 7. Schematic geometry of measurement at 77 inches distance. The horn antenna traverses the arc of the circle shown.

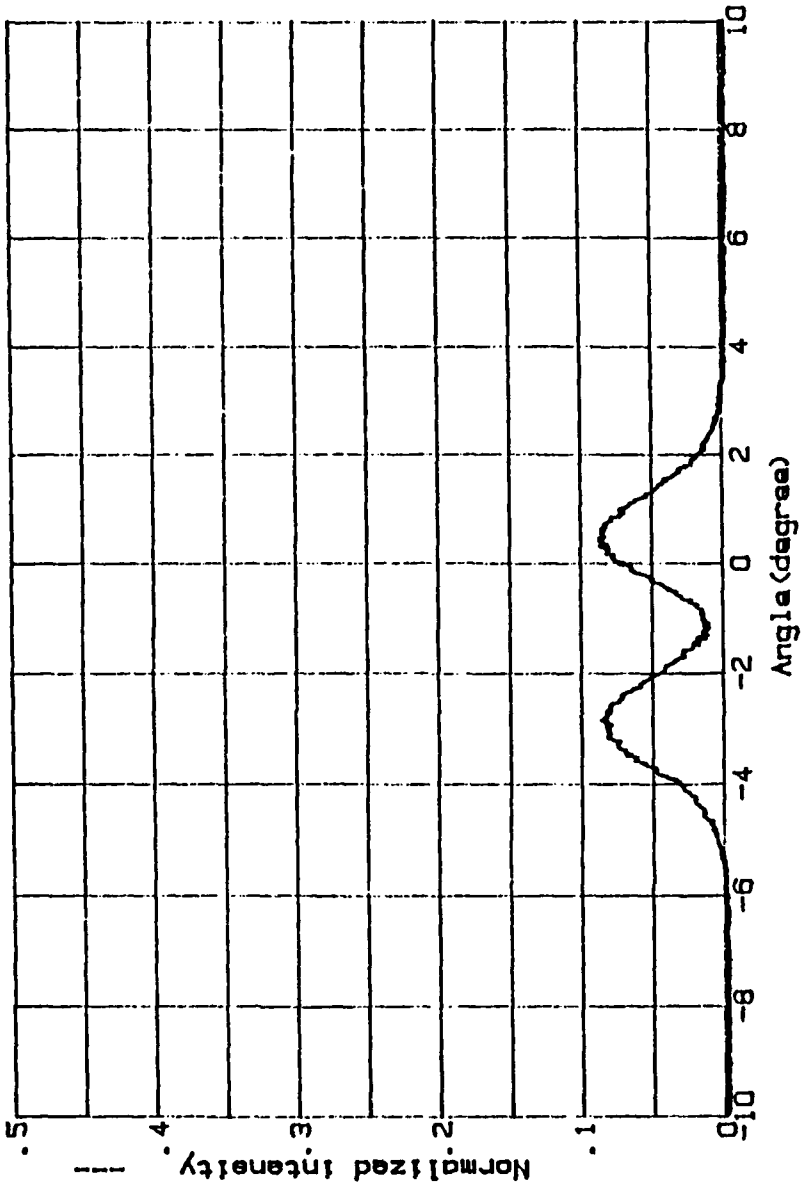

Figure 8. The Normalized Intensity of Observed Radiation versus Observed Angle. The Electron Energy is 45 MeV and the Distance from Antenna to Al plate is 77 inches

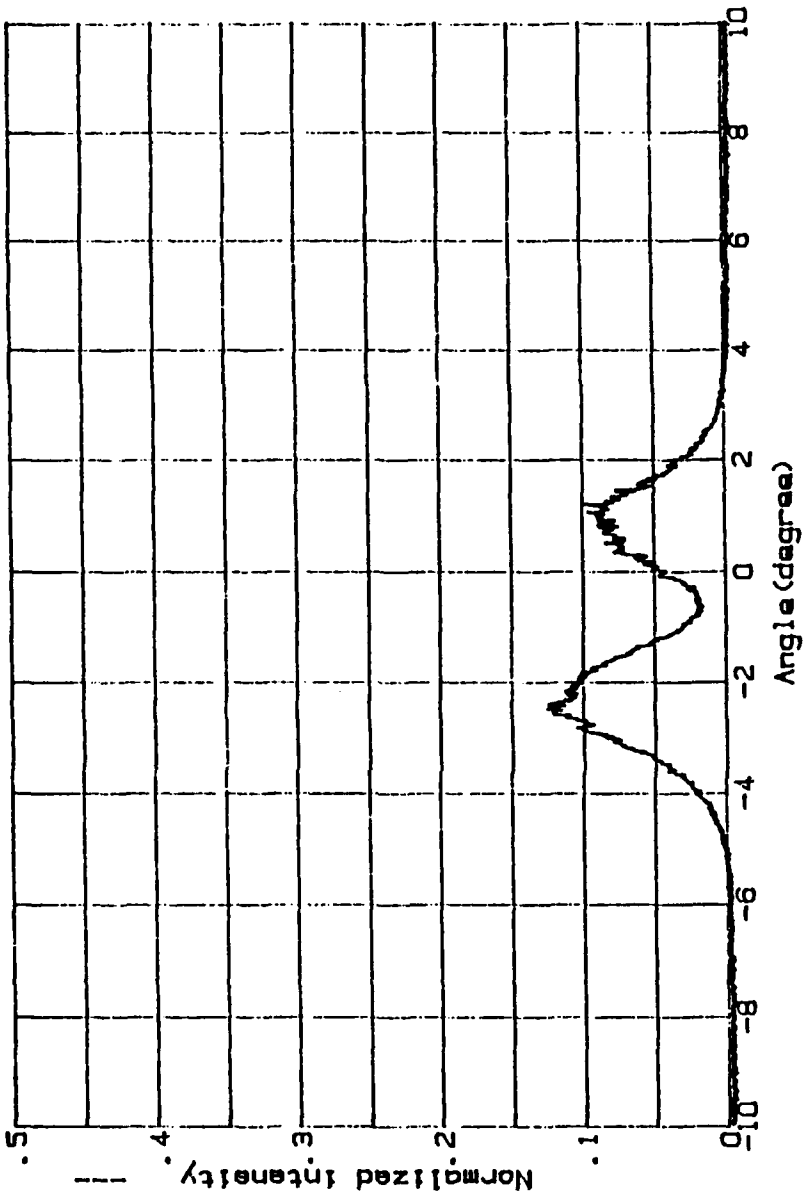

Figure 9. The Normalized Intensity of Observed Radiation versus Observed Angle. The Electron Energy is 45 MeV and the Distance from Antenna to Al plate is 58 inches

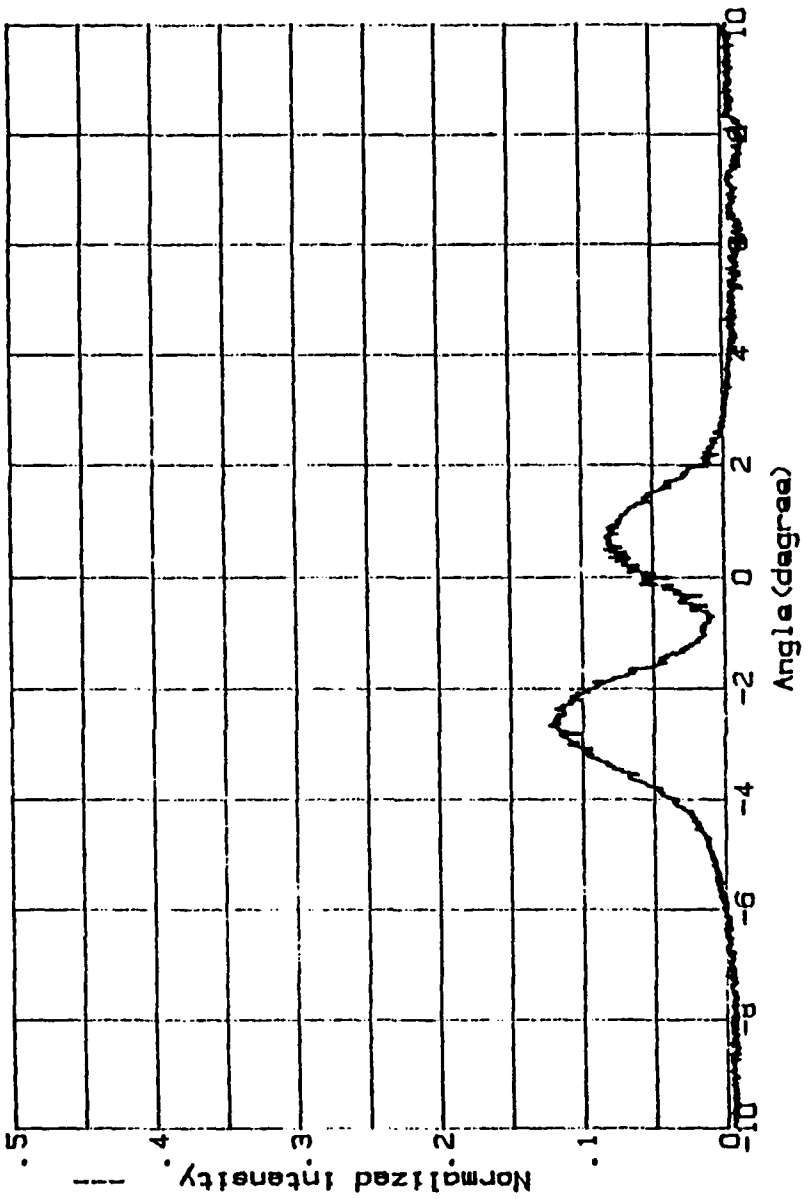

Figure 10. The Normalized Intensity of Observed Radiation versus Observed Angle. The Electron Energy is 45 MeV and the Distance from Antenna to Al plate is 48 inches

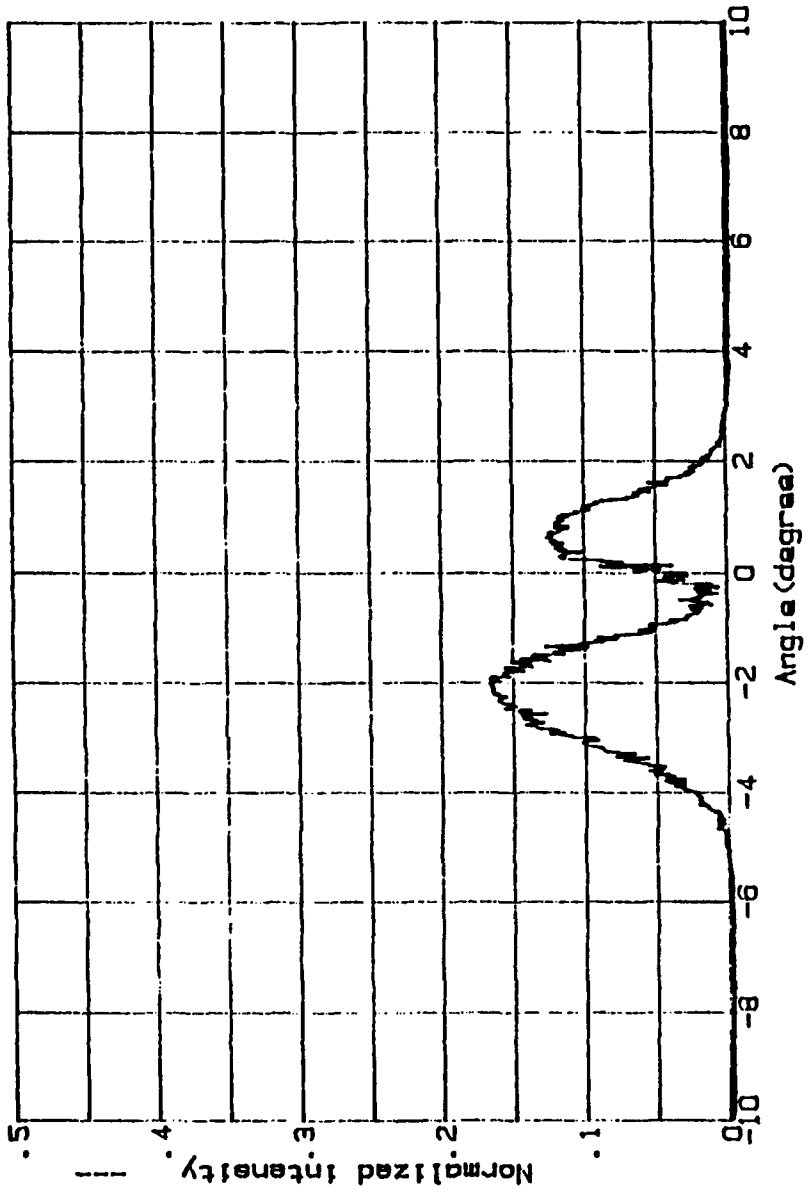

Figure 11. The Normalized Intensity of Observed Radiation versus Observed Angle. The Electron Energy is 45 MeV and the Distance from Antenna to Al plate is 38 inches

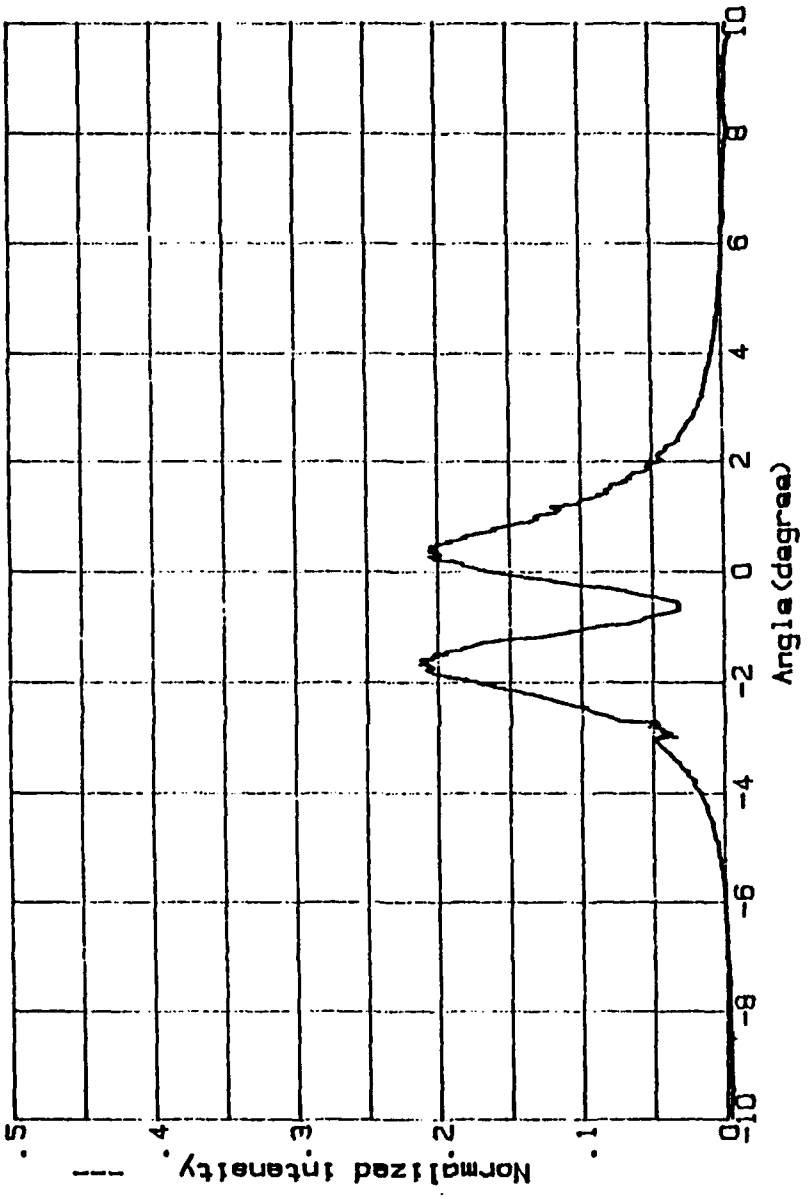

Figure 12. The Normalized Intensity of Observed Radiation versus Observed Angle. The Electron Energy is 65 MeV and the Distance from Antenna to Al plate is 77 inches

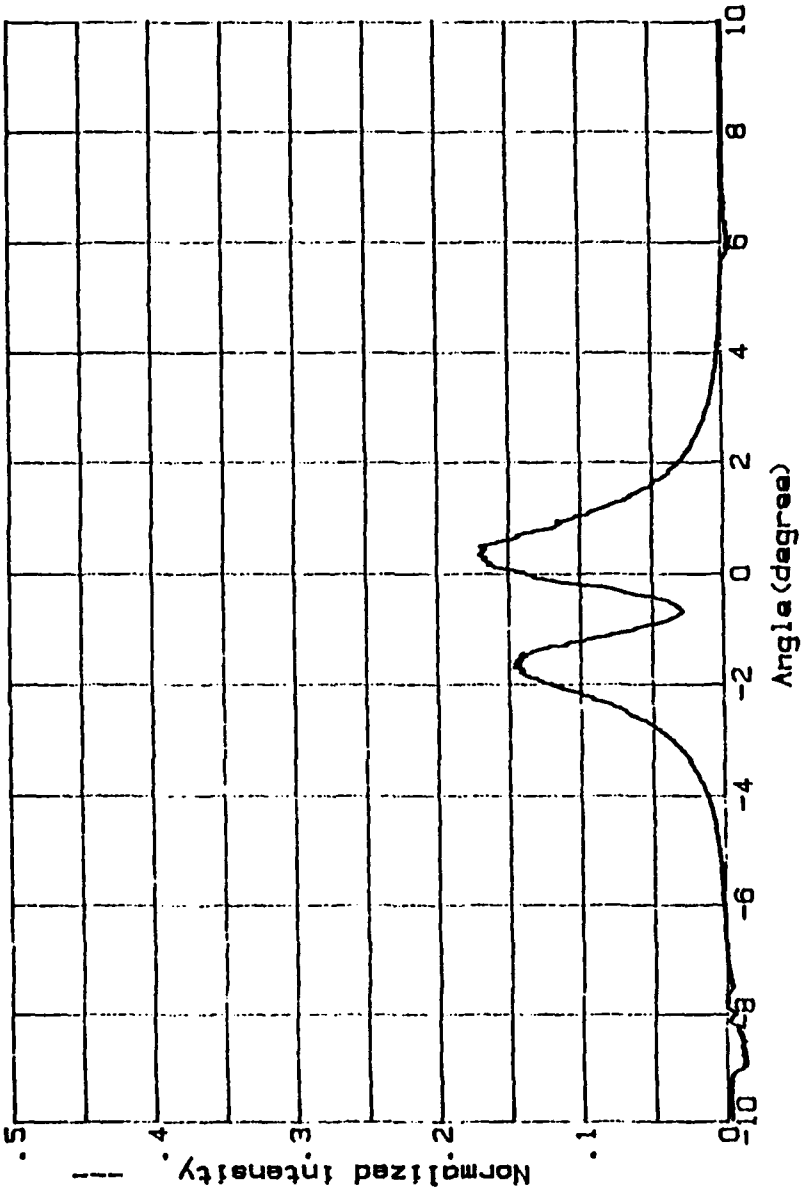

Figure 13. The Normalized Intensity of Observed Radiation versus Observed Angle. The Electron Energy is 65 MeV and the Distance from Antenna to Al plate is 58 inches

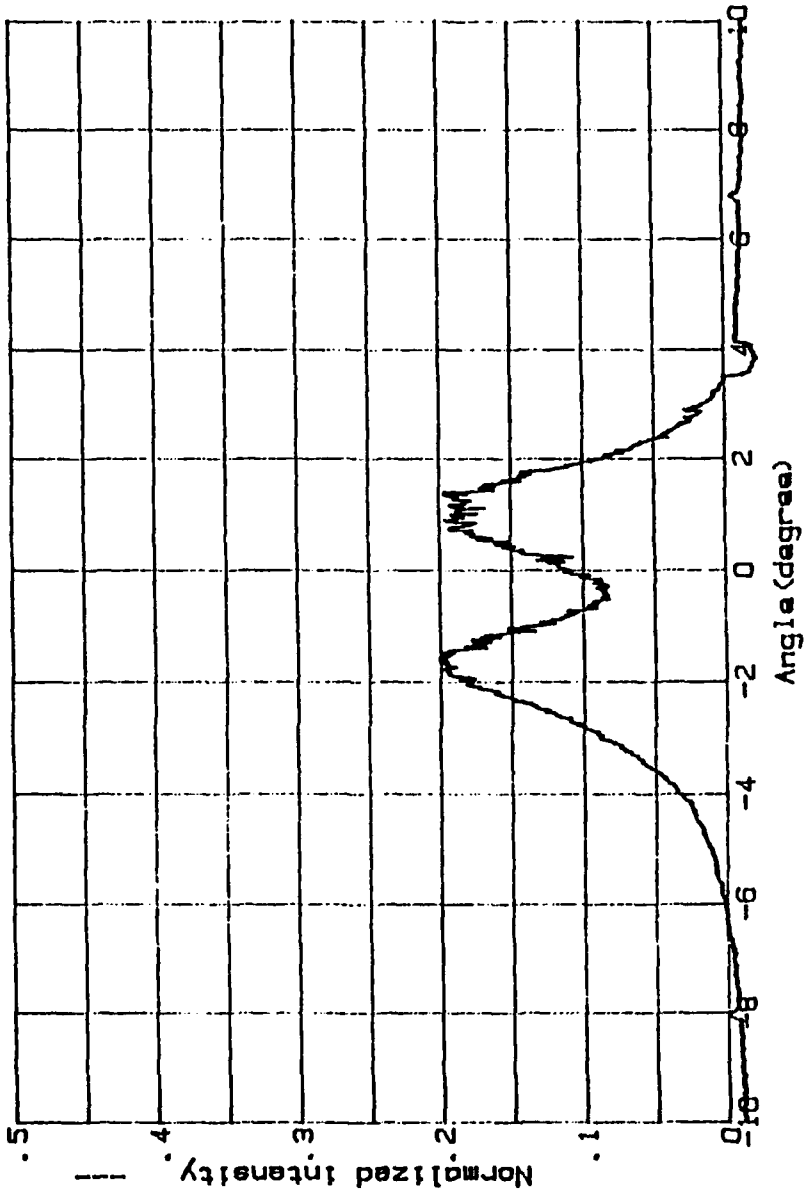

Figure 14. The Normalized Intensity of Observed Radiation versus Observed Angle. The Electron Energy is 65 MeV and the Distance from Antenna to Al plate is 48 inches

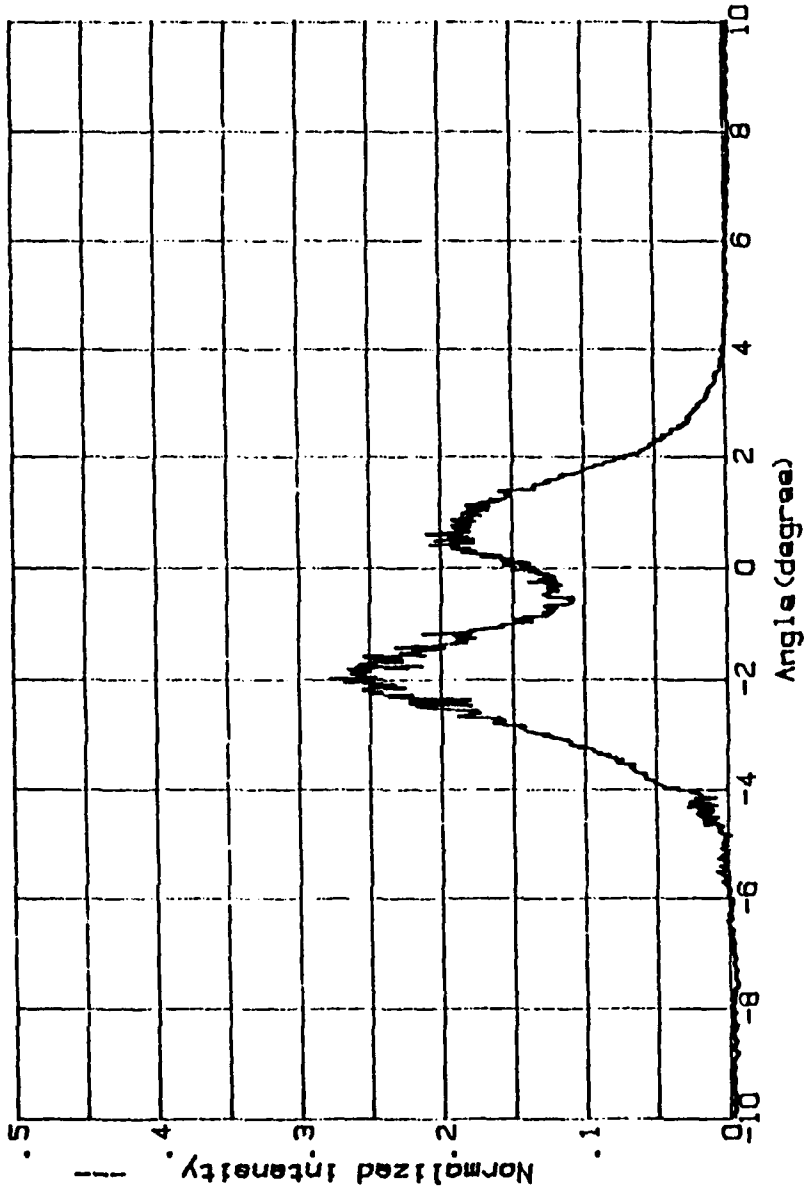

Figure 15. The Normalized Intensity of Observed Radiation versus Observed Angle. The Electron Energy is 65 MeV and the Distance from Antenna to Al plate is 38 inches

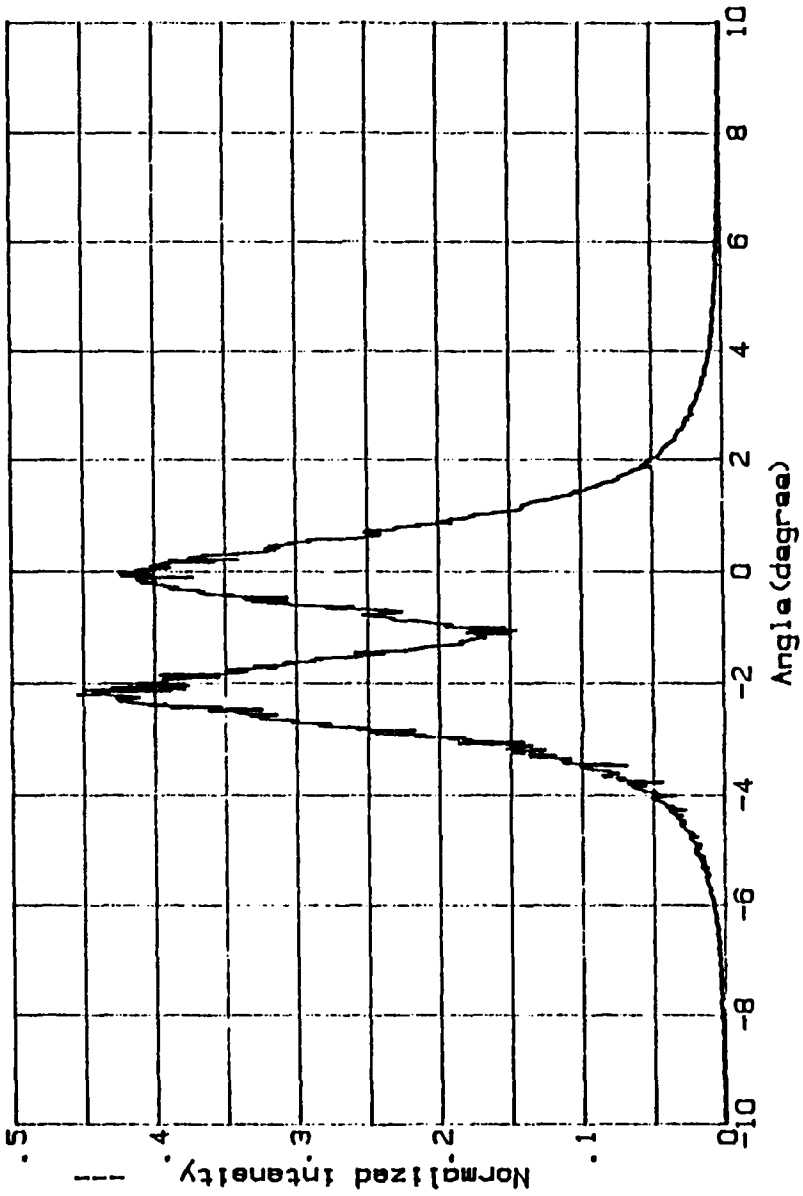

Figure 16. The Normalized Intensity of Observed Radiation versus Observed Angle. The Electron Energy is 80 MeV and the Distance from Antenna to Al plate is 77 inches

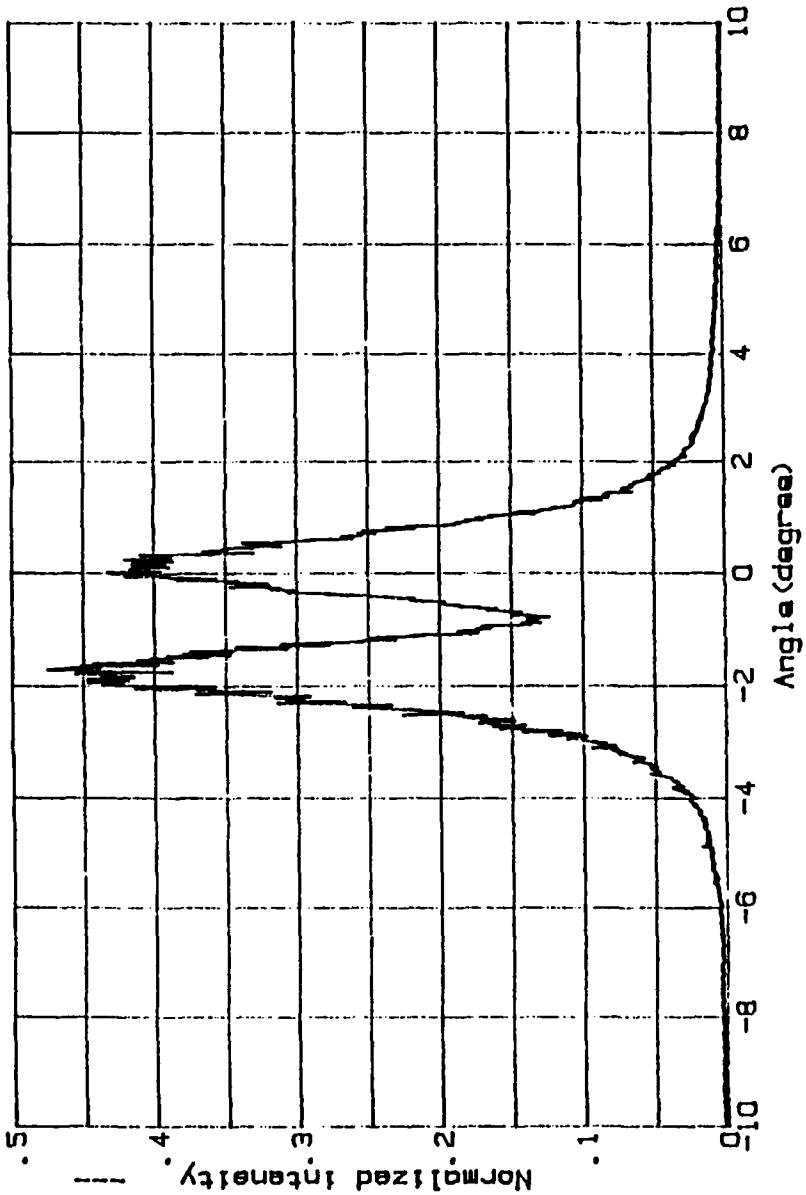

Figure 17. The Normalized Intensity of Observed Radiation versus Observed Angle. The Electron Energy is 80 MeV and the Distance from Antenna to Al plate is 58 inches

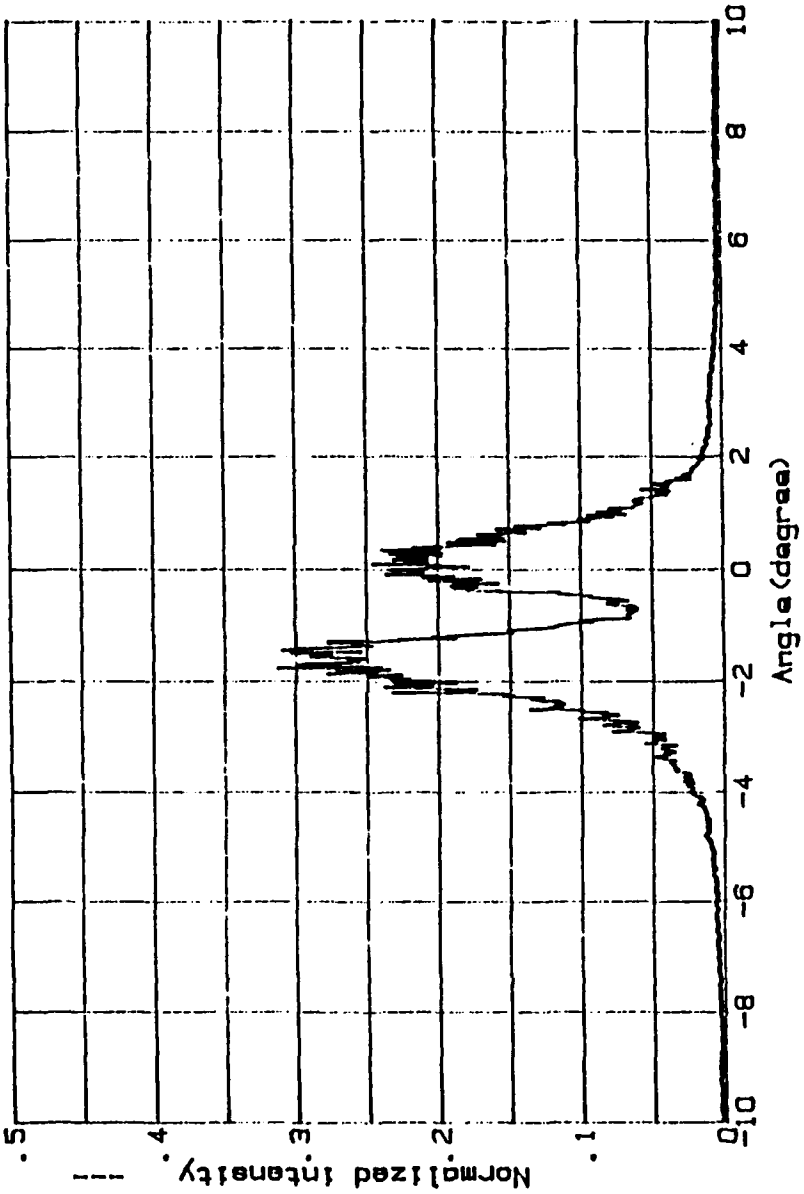

Figure 18. The Normalized Intensity of Observed Radiation versus Observed Angle. The Electron Energy is 80 MeV and the Distance from Antenna to Al plate is 48 inches

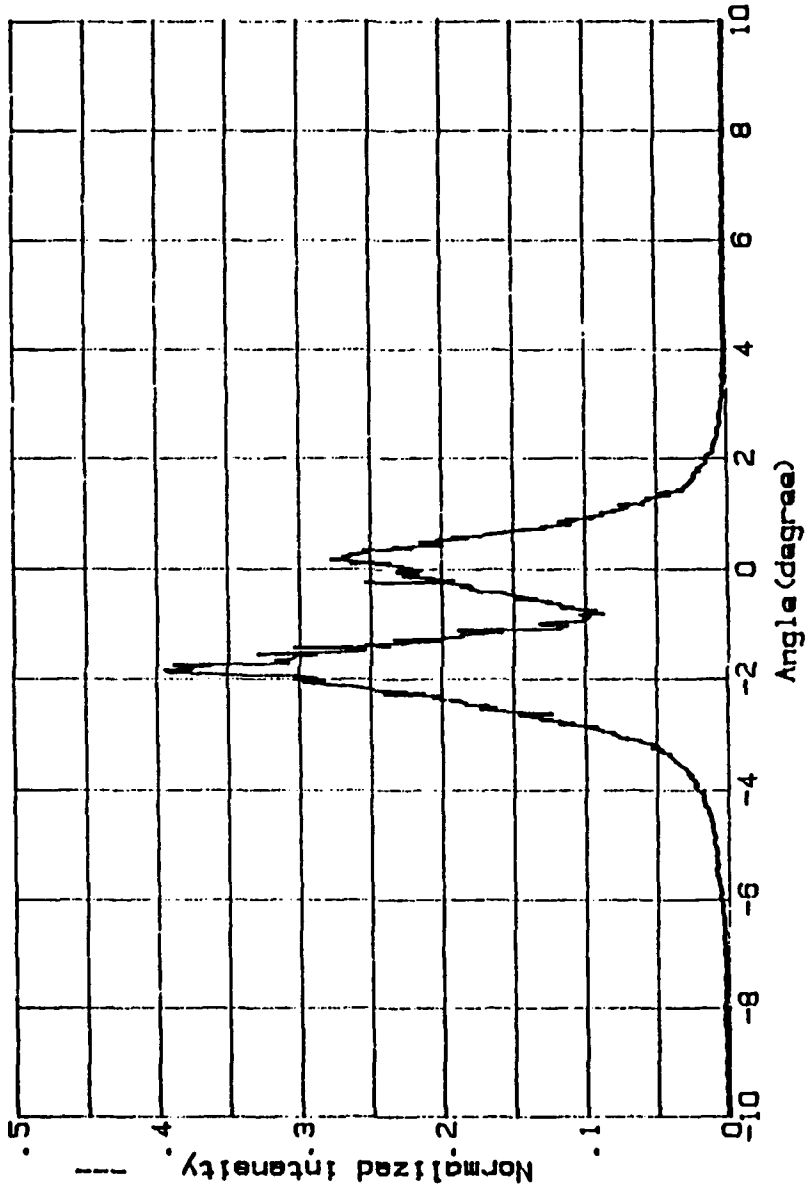

Figure 19. The Normalized Intensity of Observed Radiation versus Observed Angle. The Electron Energy is 80 MeV and the Distance from Antenna to Al plate is 38 inches

observed peak angle versus distance to foil, (3) Comparison of full width half maximum (FWHM) versus energy. The results presented are based on an empirical analysis of data. The zero position of the relative angle in these figures is an estimate, determined as half the angular distance between the peaks of the two lobe. Let's discuss more detail.

B. DISCUSSION

Although we are not currently able to explain the observed distribution of radiation, we can make some empirical observation. We discuss below (1) a comparison of the expected theoretical peak angle to the observed experimental peak angle; (2) the relationship between the measured radiation angle and the angle adjusted to the location of the aluminum foil; (3) the need for normalization of the observed radiation intensity to account for fluctuations in the electron beam intensity; (4) the behavior of the angle of the peak intensity as a function of the electron energy; and (5) the behavior of the peak intensity angle as a function of the separation distance between foil and antenna.

1. Comparison of Theoretical Angle and Experimental Angle

As we see in Table 1 and Figure 20, the observed peak angle did not correspond to the theoretical peak angles for either Cerenkov or transition radiation. There appears to be no absolute boundary between Cerenkov, transition and diffraction transition radiation, even though we tried to get an empirical separation of the three radiation by observing changes generated in the angular dependence. According to theory, the Cerenkov peak angle increases as the particle's velocity is increased, and the peak angle of TR decreases as the particle's energy is increased. But the experimental peak angle decreases as the energy increases up to certain

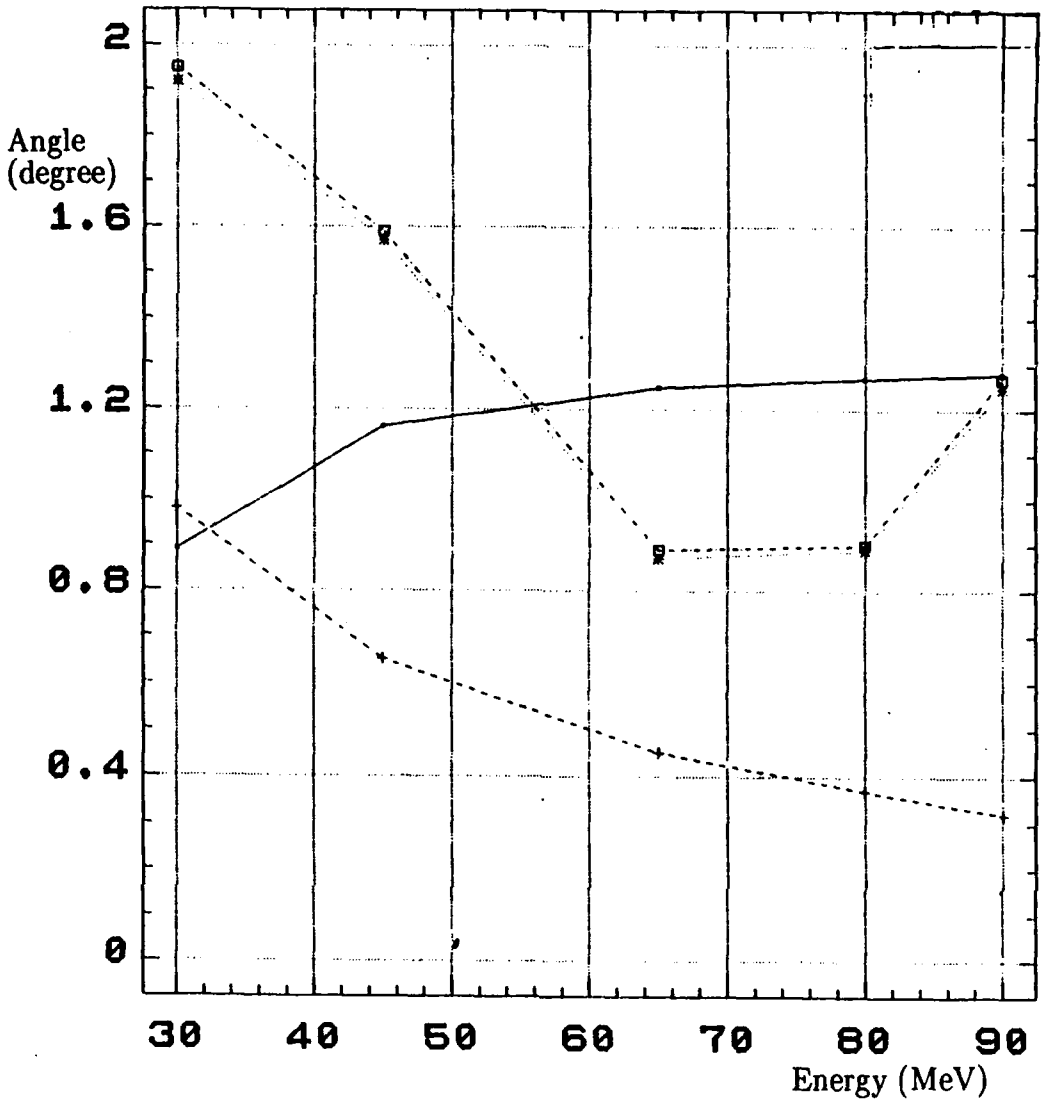

Figure 20. Theoretical Angle and Experimental Angle versus Electron Energy

Notes: + + mark stands for TR, . . mark means Cerenkov radiation in theoretical angle. * * means adjusted peak angle and [] stands for measured angle in Experiments. The distance from foil to horn is 77 inches.

extent. After that, it increases as the energy is increased. This may indicate that both Cerenkov radiation and transition radiation are present.

TABLE 1. THEORETICAL ANGLE and EXPERIMENTAL ANGLE (degree)

Index of Refraction n = 1.000268 and the distance from foil to horn is 77 inches. The angles presented are in degrees.

Name (distance in inch)	Energy (MeV)				
	30	45	65	80	90
Cerenkov	0.89	1.16	1.25	1.27	1.28
T. R.	0.98	0.65	0.45	0.37	0.32
Measured (77")	1.92	1.57	0.87	0.89	1.25
Adjusted (77")	1.95	1.59	0.89	0.90	1.27

2. Measured Angle and Adjusted Angle

The measured angle for the horn antenna as seen in Figure 7 is not the angle from the horn antenna to the beam line at the aluminum plate location. The measured angle was adjusted to account for the dislocation of the horn lever arm. See Figure 7. Therefore the measured angle must be converted to the adjusted angle where the Al foil is located. We show the measured angle in Table 2 and the adjusted angle in Table 3. When the Al foil is located outside of the lever arm, the adjusted angle is smaller than the measured angle because of the geometry, and if it is located inside of the arm, the adjusted angle is greater than the measured angle (refer to Figure 7). In further discussion, the peak angle refers to the adjusted angle.

TABLE 2. MEASURED ANGLE

The angle presented is in degrees. The distance is from foil to horn.

Distance (inch)	Energy (MeV)				
	30	45	65	80	90
77	1.95	1.59	0.89	0.90	1.27
58	1.95	1.62	0.91	0.75	1.21
48	1.86	1.53	0.92	0.76	1.28
38	1.73	1.22	0.87	0.82	1.06

TABLE 3. ADJUSTED ANGLE

The angle presented is in degrees. The distance is from foil to horn.
Comparing to TABLE 2, adjusted angle is smaller than the measured angle at 77 inches and after that, adjusted angle is larger than the measured angle.

Distance (inch)	Energy (MeV)				
	30	45	65	80	90
77	1.92	1.57	0.87	0.89	1.25
58	2.55	2.17	1.18	0.99	1.58
48	2.94	2.42	1.46	1.20	2.03
38	3.46	2.45	1.73	1.63	2.12

The difference between the measured and the adjusted angles are slight for the 77 inch distance (see Figure 20) and largest for the 38 inch distance.

3. Normalization of the Observed Radiation Intensity

The radiation observed by the antenna horn must be normalized to account for fluctuations in the beam intensity. In Figure 21, beam intensity and raw data are very unstable and as a result, it is difficult to determine the peak angle. When the raw data is normalized to the beam intensity, the radiation peak is clearly determined. In Figure 22, the beam intensity and raw data are almost stable and as a result the peak angles can be determined from raw data. Normalization enhances the angular location of the peaks. These two example data illustrate the need for normalization of the raw antenna signal.

4. Peak Angle versus Electron Energy

The relation between peak angle and energy is shown in Table 4 and Figure 23. When the location of the thin aluminum foil is fixed, the peak angle

TABLE 4. PEAK ANGLE versus ELECTRON ENERGY

The angle presented here is in degrees and the distance is from foil to horn.

Distance (inch)	Energy (MeV)				
	30	45	65	80	90
77	1.92	1.57	0.87	0.89	1.25
58	2.55	2.17	1.18	0.99	1.58
48	2.94	2.42	1.46	1.20	2.03
38	3.46	2.45	1.75	1.63	2.12

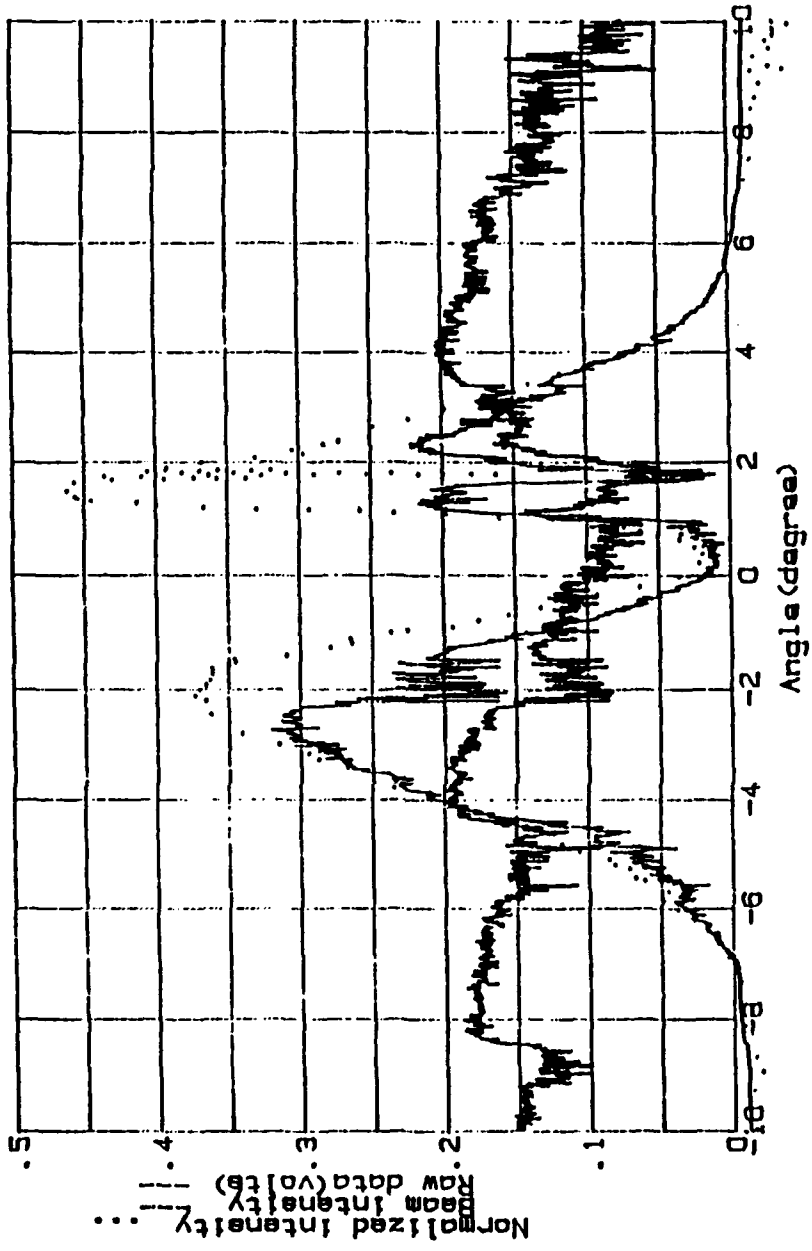

Figure 21. Normalization with Bad Raw Data

... is normalized intensity, —— (thin line) is raw data from movable horn and ——— (thick line) is beam intensity from fixed horn.

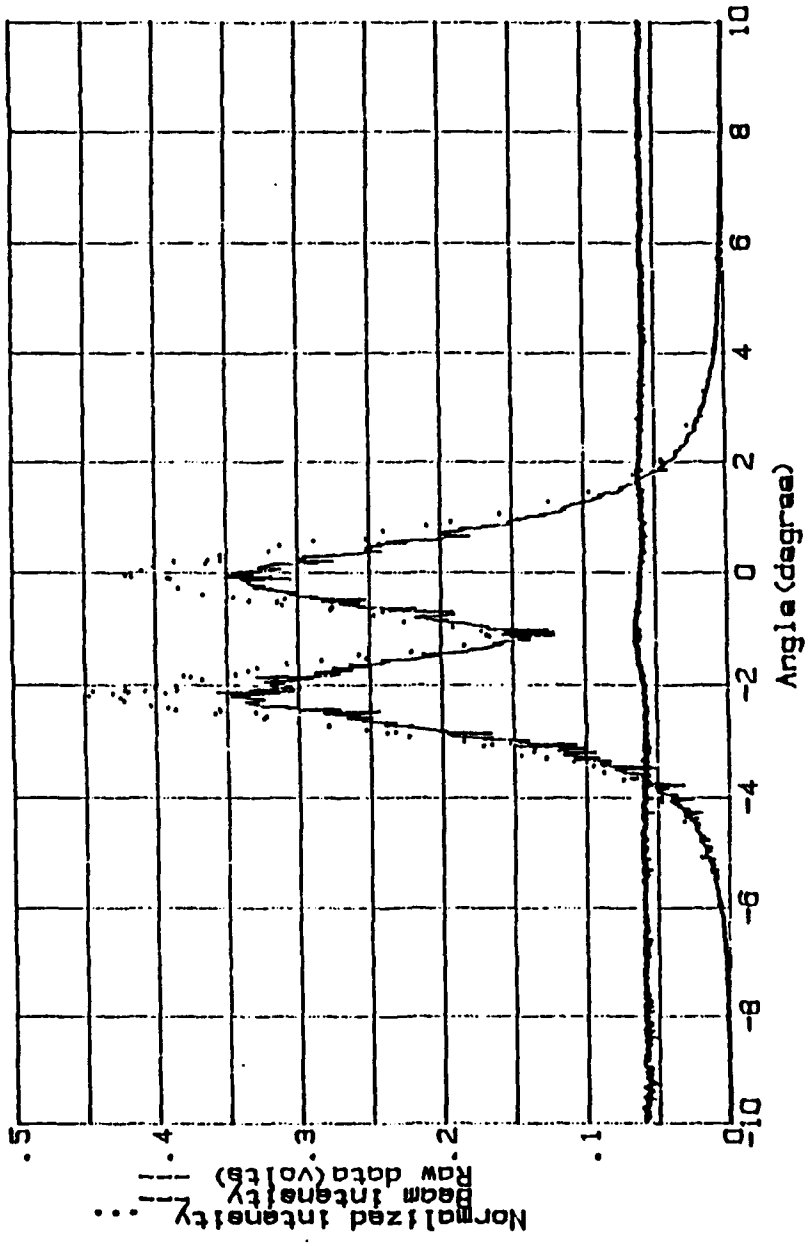

Figure 22. Normalization with Good Raw Data

... is normalized intensity, —— (thin line) is raw data from movable horn and —— (thick line)is beam intensity from fixed horn.

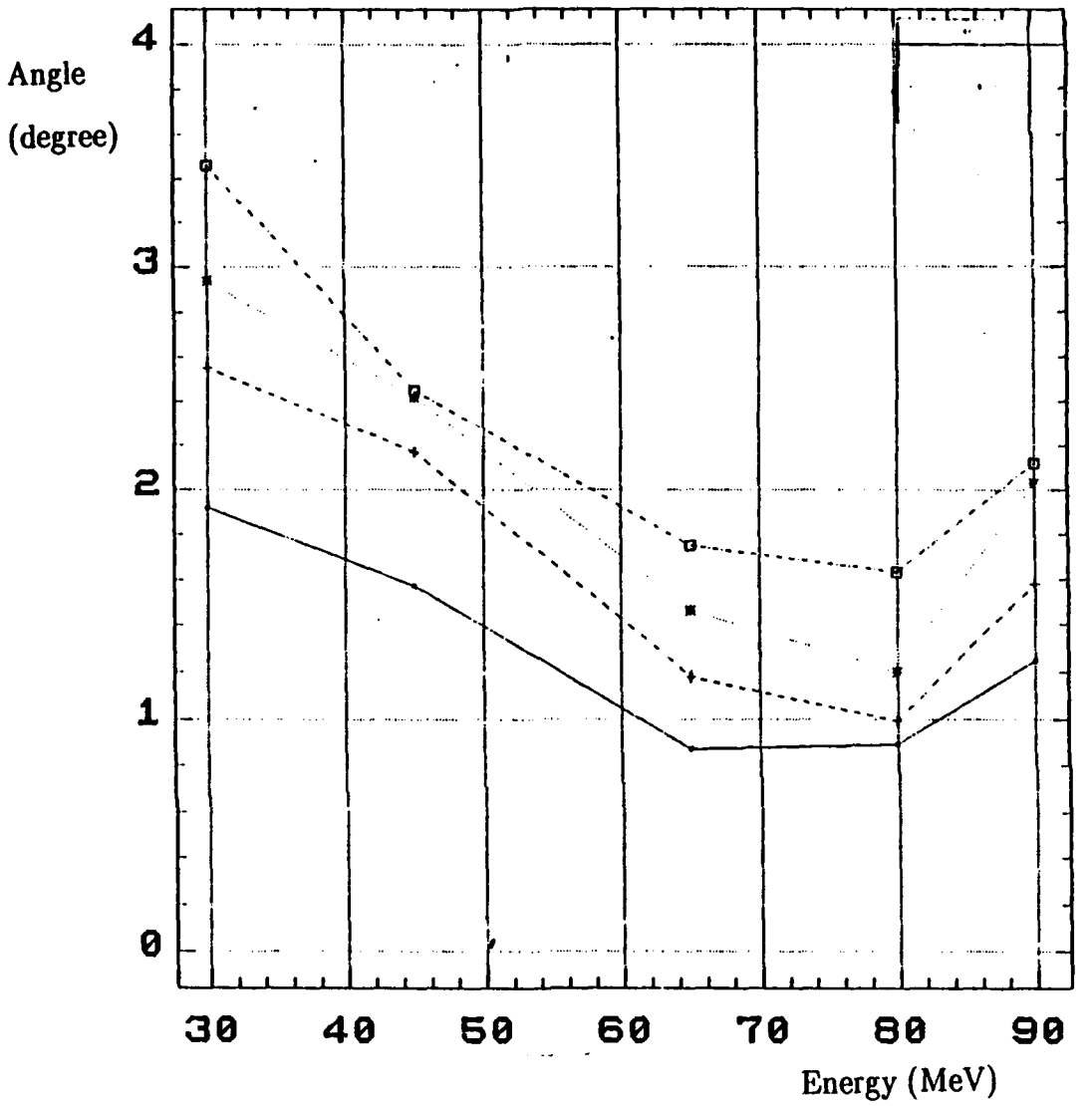

Figure 23. Peak Angle versus Electron Energy

Notes: .. is come from 77 inches distant from Al foil to arc of lever arm

,+ + from 58 inches, * * from 48 inches and [] from 38 inches.

decreases with increasing beam intensity up to approximately 70 or 80 MeV, then begins to increase as the beam energy is further increased. The peak angle also decreases. as the distance between the position of aluminum foil and arc of lever arm decreases.

According to the theory of Cerenkov radiation, the intensity depends on the speed of the charged particle. This peak angle occurs at $\cos \theta_c = \frac{c'}{v} = \frac{1}{n\beta}$. With the same index of refraction, β increases as the energy increases and therefore the peak angle becomes larger with increasing energy. According to the theory of transition radiation, the intensity depends upon the energy of the charged particle. The peak angle occurs at $\theta_p = \gamma^{-1}$. The Lorentz factor γ increases as the beam energy increases. Therefore the peak angle should decrease with increasing beam energy.

In Figure 23, the peak angle of the charged particle decreases as the energy increases up to approximately 80 MeV. This is characteristic of TR and DTR. The peak angle increases as increasing the energy after about 80 MeV. This behavior is characteristic of Cerenkov radiation. Therefore we suspect that both TR and Cerenkov radiation are being generated. We may be observing mostly TR at lower energies and Cerenkov radiation at higher energies.

5. Peak Angle versus Distance between Foil and Antenna

We now compare the peak angle to the distance between the foil and the antenna. According to Table 5 and Figure 24, the peak angle gets smaller as the distance between the position of aluminum foil and arc of lever arm increases. The decrease in peak angle is almost linear with the foil–antenna separation distance.

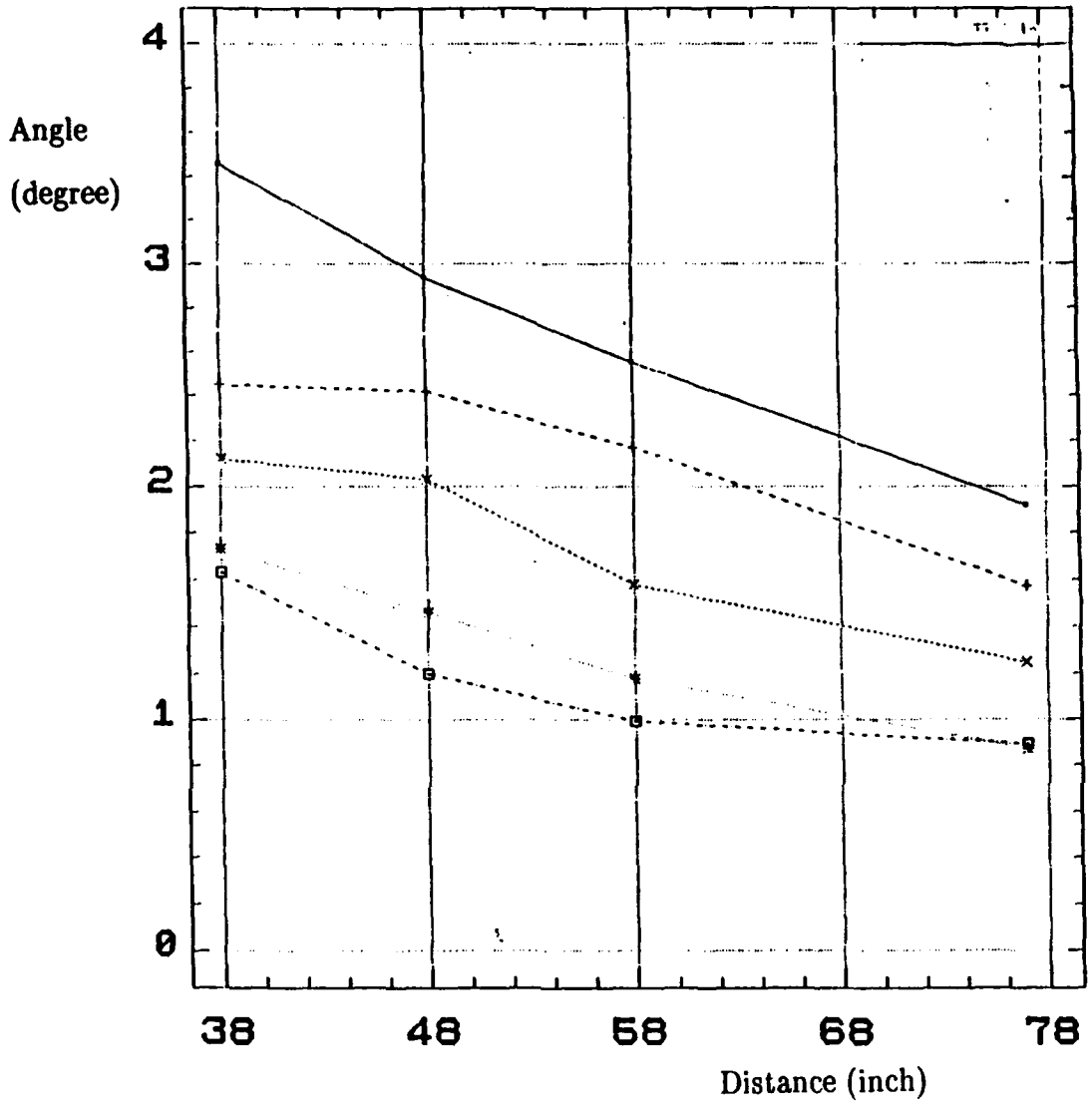

Figure 24. Peak Angle versus Distance

Notes: ..is come from at 30 MeV electron energy, + + at 45 MeV, x x at 90 MeV, * * at 80 MeV and [] at 65 MeV.

TABLE 5. PEAK ANGLE versus DISTANCE

The angle presented here is in degrees and distance is from foil to horn.

Energy (MeV)	Distance (inch)			
	77	58	48	38
30	1.92	2.55	2.94	3.46
45	1.57	2.17	2.42	2.45
65	0.87	1.18	1.46	1.73
80	0.89	0.99	1.20	1.63
90	1.25	1.58	2.03	2.12

6. Width of the Intensity Lobes

We define the full width half maximum (FWHM) of the peak intensity lobes in Figure 25. The relation of the FWHM to energy is given in Table 6, 7, 8 and Figure 26. In general the peak width decreases as the energy increases up to about 80 MeV, and increases sharply as the energy is increased further. For a given energy,the peak width increases with increasing separation distance between the aluminum foil and the antenna horn. This general behavior applies to both the right and left lobes and to the combined width of the two lobes (total width defined in Figure 25). Qualitatively, the decrease of lobe width with energy up to about 80 MeV and the increase after 80 MeV is similar to the behavior of the peak angle, as discussed in section 4 above.

TABLE 6. FWHM (left lobe) versus Electron Energy

The angle presented here is in degrees and distance is from foil to horn.

Distance (inch)	Energy (MeV)				
	30	45	65	80	90
77	0.65	0.53	0.42	0.42	0.62
58	0.73	0.52	0.38	0.36	0.59
48	0.66	0.54	0.39	0.30	0.68
38	0.58	0.54	0.40	0.32	0.64

TABLE 7. FWHM (right lobe) versus Electron Energy

The angle presented here is in degrees and distance is from foil to horn.

Distance (inch)	Energy (MeV)				
	30	45	65	80	90
77	0.61	0.51	0.41	0.45	0.61
58	0.75	0.42	0.37	0.35	0.65
48	0.69	0.51	0.38	0.25	0.39
38	0.58	0.46	0.39	0.31	0.71

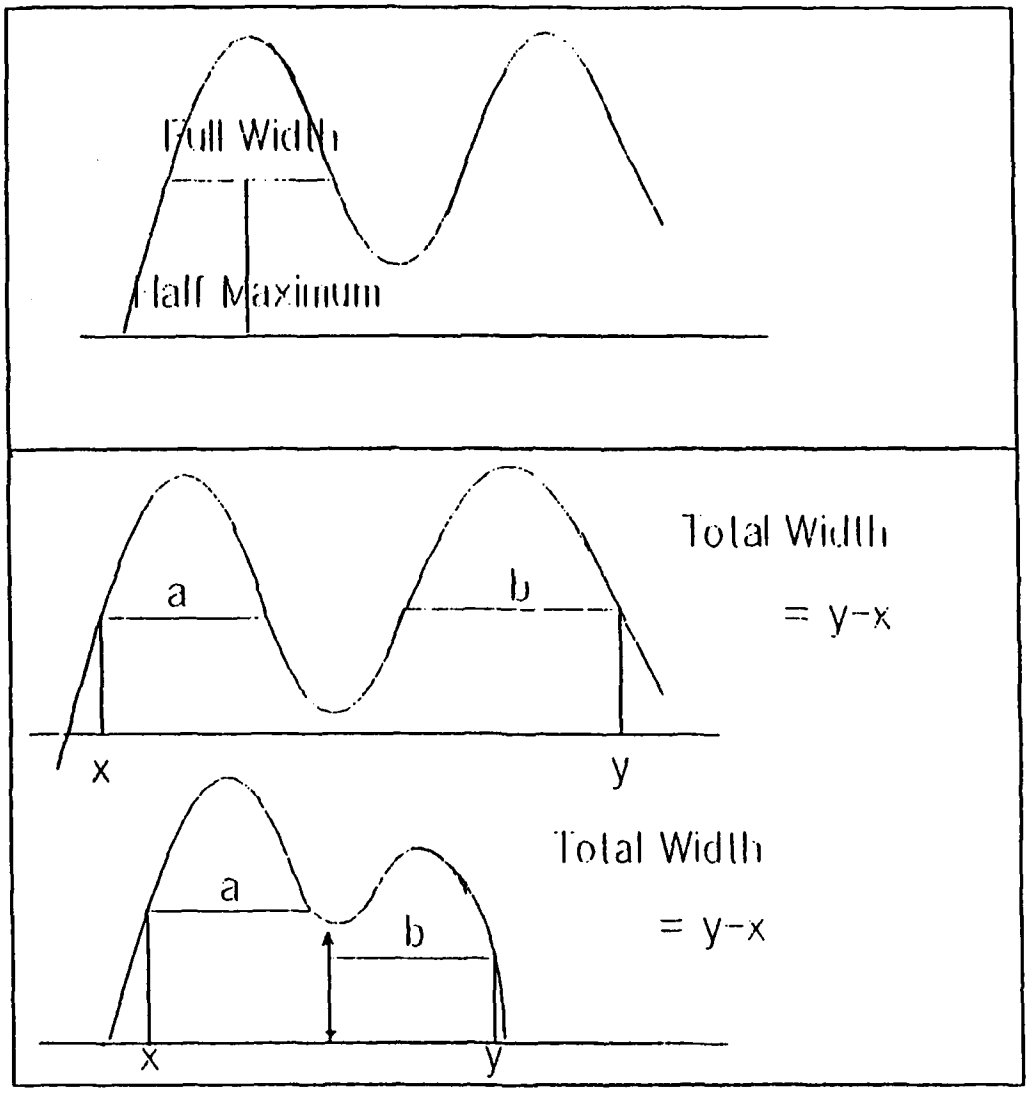

Figure 25. Definition of FWHM

The full width half maximum of the left or right lobes are defined in the conventional manner. The total width is the angular distance between the left edge of the full width half maximum of the left lobe (position x) to the right edge of the full width half maximum of the right lobe (position y).

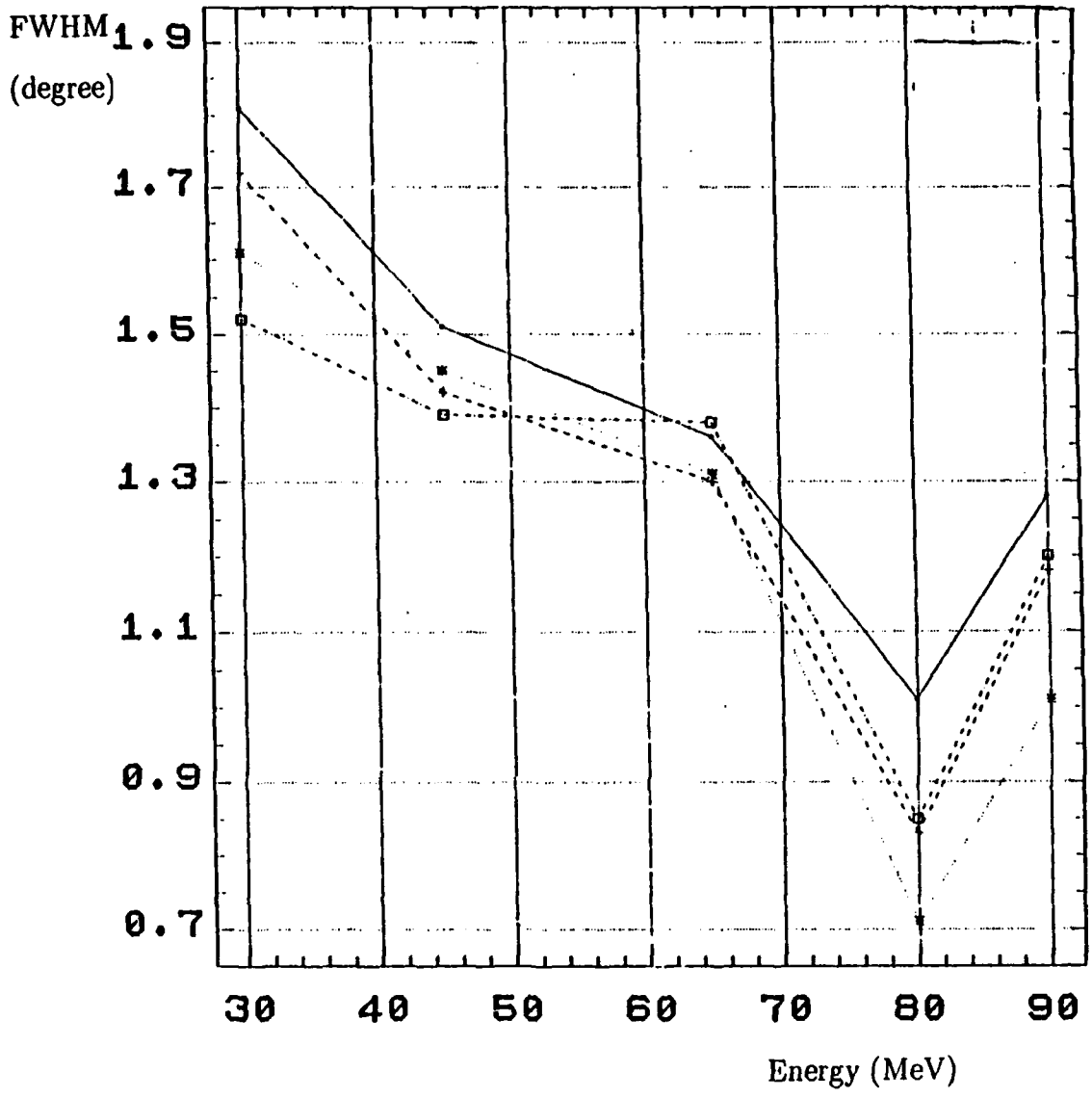

Figure 26. FWHM (total width) versus Electron Energy

Notes: [] [] is come from 38 inches distant from Al foil to arc of lever arm,

* * from 48 inches, + + from 58 inches, . . from 77 inches.

TABLE 8. FWHM (total width) versus Electron Energy

Angle presented here is in degrees and distance is from foil to horn.

Distance (inch)	Energy (MeV)				
	30	45	65	80	90
77	1.81	1.51	1.36	1.01	1.28
58	1.72	1.42	1.30	0.83	1.18
48	1.61	1.45	1.31	0.71	1.01
38	1.25	1.31	1.38	0.85	1.20

IV. CONCLUSIONS

We have observed x–band radiation which occurs when an electron beam travelling in air traverses an aluminum plate. The radiation pattern is more complicated than can be explained with a simplified model of Cerenkov radiation from an infinite interaction length and transition radiation from the aluminum–air interface. The empirical observation is that the peak angle decreases with energy until about 70 MeV, then increases with energy. The angular width of the peak distribution shows a similar behavior with energy. The observed peak angle decreases as the distance from the horn antenna to the aluminum foil is increased. The explanation of the radiation distribution observed is not yet satisfactory. We believe that we are seeing the combined effects of both Cerenkov and transition radiation.

A major improvement in the data accumulation process has been introduced by measuring radiation at a fixed angle with one horn as data is taken with a second movable horn. This procedure allows us to compensate for the fluctuating electron beam intensity. The data can now be digitized and stored in a computer for analysis. Previous experiments allowed only for analog measurements.

Further work, both theoretical and experimental, will be required to understand fully the radiation signature of the electron beam.

APPENDIX A

OPERATING CHARACTERISTICS of THE NPS LINAC

1. Beam energy ..... 15 MeV – 100 MeV
2. Beam micro bunch length ..... 0.0024 m
3. Beam micro bunch distance ..... 0.103 m
4. Beam micro bunnch charge ..... 1.16×10^{-12} c
5. Third harmonic frequency ..... 8.568 GHz
6. Third harmonic wavelength ..... 3.5 cm

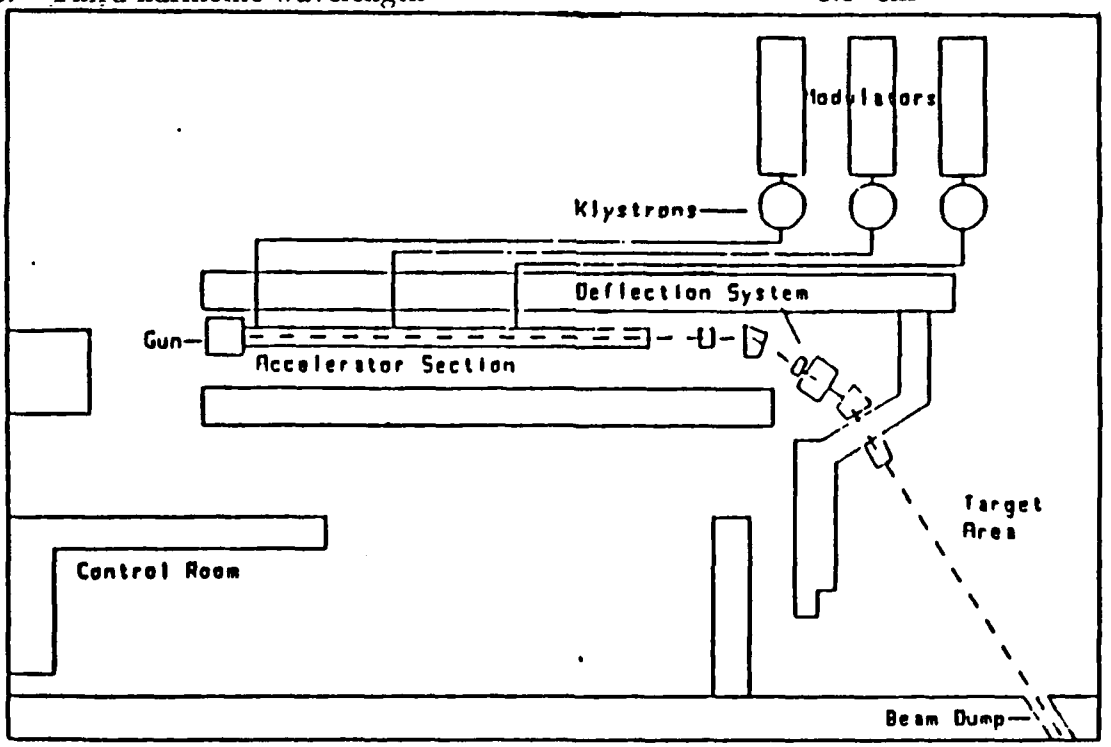

Figure 27. Experimental Station

APPENDIX B

PROGRAM FOR THE NORMALIZED INTENSITY and RAW DATA

```
10    !This program provides a normalized radiation with a toroid
20    !on the beam pipe and moving horn antenna.
30    !Plotting is provided by HP 7090A.
40    !
50    !Main program
60    ASSIGN @Hp7090 TO 705
70    OPTION BASE 1
80    !
90    !Define the variables.
100   REAL Chan1(1:1000),Chan3(1:1000),Normal(1:1000)
101   REAL Beam(1:1000),Signa(1:1000),Devide(1:1000)
110   INTEGER I,N,Factor
120   !
121   LINPUT "Do you run machine?",Answer$
122   IF Answer$="N" THEN 291
123   !
130   !Set initial conditions for the plotter.
140   OUTPUT @Hp7090;"RE11;"      !select channel 1 and 3 vs. time
150   OUTPUT @Hp7090;"IR.5,0,.5;"  !.5 volts scale for each channel
160   OUTPUT @Hp7090;"TB18,0;"    !sets total time to 18 seconds
170   OUTPUT @Hp7090;"IP1750,2300,9250,7150;"
171   OUTPUT @Hp7090;"IZ1750,2300,9250,7150;"
172   OUTPUT @Hp7090;"SC0,1000,0,1000;"
180   !
190   !Takes data into buffers through 2 channels.
200   DISP "PRESS FILL BUFFER. IF FILLED, THEN PRESS CONTINUE,"
210   PAUSE
220   WAIT .5
230   !
240   !
250   !Subprogram command
260   GOSUB Data_trans
280   GOSUB Plot_data
290   GOSUB Save_data
291   LINPUT "DO YOU WANT TO DRAW RAW DATA USING BDAT FILE ?",Answer$
292   IF Answer$="N" THEN 295
293   GOSUB Load_data
294   GOSUB Plotting
295   LINPUT "Do you want to draw normal using BDAT file ?",Answer$
```

```
296    IF Answer$="N" THEN 300
297    GOSUB Load_data
299    GOSUB Normalization
300    GOSUB Draw_area
302    DISP "PLOTTING IS COMPLETE."
303    STOP
310    !
320    !
330    !Group of subprogram
340 Data_trans: !This subroutine takes data from 2 buffers
350             !and stores in array variables Chan1 and 3.
360             !
370             !Transfer channel 1 data to Chan1 array.
380                DISP "TRANSFERRING DATA"
390                OUTPUT @Hp7090;"DO1,1000,0,0;"
400                OUTPUT @Hp7090;"QI;"
410                FOR N=1 TO 1000
420                ENTER @Hp7090 USING "#,K";Chan1(N)
430                NEXT N
440             !
450             !Transfer channel 3 data to Chan3 array.
460                OUTPUT @Hp7090;"DO3,1000,0,0;"
470                OUTPUT @Hp7090;'QI;"
480                FOR N=1 TO 1000
490                ENTER @Hp7090 USING "#,K";Chan3(N)
500                NEXT N
510                RETURN
520             !
530             !
690 Plot_data:  !This subroutine plots the normalized transition
700             !
710                GOSUB Normal                !normalize the data
720                DISP "NORMALIZED PATTERN IS DRAWING."
730             !
740             !Sets scale factor 1000, 1000 for X and Y-axis
750                OUTPUT @Hp7090;"SC0,1000,0,1000;"
760             !
770             !Select pen 3 and line type
780                OUTPUT @Hp7090;"SP5;LT;"
790             !
800             !Transfer normalized data from computer to plotter
810             !Set ratio 400% and drawing data
820                Factor=400                  !ratio (1000/2,5)
830                FOR N=1 TO 1000
840                IF N=1 THEN OUTPUT @Hp7090;"PUPA";N;Normal(N)*Factor
850                OUTPUT @Hp7090;"PDPA";N;Normal(N)*Factor
860                NEXT N
```

```
870                 OUTPUT @Hp7090;"PU;SC;IW;"
880                 DISP "PLOTTING IS COMPLETE."
890                 RETURN
900               !
910               !
920 Normal:       !This program make a normalization for Chan1 and Chan2.
930               !Chan1 is a toroid and Chan2 is a moving antenna.
940               !
950                 DISP "NORMALIZING TRANSITION PATTERN."
960                 FOR I=1 TO 1000
970                   IF Chan1(I)=0 THEN          !avoid 0 value
980                     Chan1(I)=Chan1(I+1)
990                     Chan3(I)=Chan3(I+1)
1000                  END IF
1010                  Normal(I)=Chan1(I)/Chan3(I)
1020                NEXT I
1030                RETURN
1040              !
1050              !
1060 Save_data:   !This subprogram save the data into separated file
1070              !which name is given by you.
1080              !
1090              !Save the beam data
1100                LINPUT "DO YOU WANT SAVE THE DATA ?",Answer$
1110                IF Answer$="N" THEN 1220
1120                LINPUT "ENTER FILE NAME TO STORE DATA: ",Name$
1130                MASS STORAGE IS ":,4,1"     !left drive as MSI
1140                CREATE BDAT Name$,3000,8    !3000 real numbers
1150                ASSIGN @Path TO Name$       !assign I/O path
1160                OUTPUT @Path;Chan1(*)       !send Chan1 data
1170                OUTPUT @Path;Chan3(*)       !send Chan3 data
1180                OUTPUT @Path;Normal(*)      !send Normal data
1190                ASSIGN @Path TO *           !close I/O path
1200                MASS STORAGE IS ":,4,0"     !return to right drive
1210                DISP "COMPLETE SAVING DATA."
1220                RETURN
1221    !This program is used to redraw the data in BDAT files.
1222    !BDAT files store the data obtained using "NORMAL" program.
1230 Load_data:!THIS PROGRAM LOAD THE DATA FROM BDAT FILE
1240            !into the program
1250            !
1260            MASS STORAGE IS ":,4,1"       !left drive as MSI
1270            LINPUT "ENTER A BDAT FILE NAME :",File$
1280            DISP "TRANSFERRING DATA FROM ";File$
1290            ASSIGN @Path TO File$         !connect to file
1300            ENTER @Path;Beam(*)           !load beam data
1310            ENTER @Path;Signa(*)          !load signal data
1320            ENTER @Path;Devide(*)
```

```
1330            PRINTER IS 701
1340            FOR I=1 TO 1000 STEP 99.9
1350            PRINT I,Signa(I),Beam(I),Devide(I)
1360            NEXT I
1370            PRINTER IS 1
1380            ASSIGN @Path TO *           !close the path
1390            MASS STORAGE IS ":,4,0"     !right drive as MSI
1400            RETURN
1410            !
1420 Plotting:  !This subprogram plots the beam pattern.
1430            !
1440            DISP "BEAM PATTERN PLOTTING"
1450            OUTPUT @Hp7090;"IP1750,2300,9250,7150;"
1460            OUTPUT @Hp7090;"IZ1750,2300,9250,7150;"
1470            OUTPUT @Hp7090;"SC0,1000,0,1000;"
1480            OUTPUT @Hp7090;"SP1,LT;"
1490            FOR N=1 TO 1000
1500               IF N=1 THEN OUTPUT @Hp7090;"PUPA";N;Beam(N)*1500
1510               OUTPUT @Hp7090;"PDPA";N;Beam(N)*1500
1520            NEXT N
1530            OUTPUT @Hp7090;"PU;"
1540            !
1550            !
1560            !This subprogram plots the detected signal
1570            OUTPUT @Hp7090;"SP2,LT;"
1580            FOR N=1 TO 1000
1590                IF N=1 THEN OUTPUT @Hp7090;"PUPA";N;Signa(N)*1500
1600                OUTPUT @Hp7090;"PDPA";N;Signa(N)*1500
1610            NEXT N
1620            RETURN
1630            !
1631 Normalization:!This subroutine plots the normalization by using
1632                !BDAT file which is DEVIDE.
1633                DISP "Normalization pattern is drawing."
1634                OUTPUT @Hp7090;"IP1750,2300,9250,7150;"
1635                OUTPUT @Hp7090;"IZ1750,2300,9250,7150;"
1636                OUTPUT @Hp7090;"SC0,1000,0,1000;"
1637                OUTPUT @Hp7090;"SP5,LT;"
1638                FOR N=1 TO 1000
1639                    IF N=1 THEN OUTPUT @Hp7090;"PUPA";N;Devide(N)*200
1640                    OUTPUT @Hp7090;"PDPA";N;Devide(N)*200
1641                NEXT N
1643                RETURN
1645 Draw_area:!Define drawing area,grid and pen
1650            DISP "DRAWING PLOT AREA"
1660            OUTPUT @Hp7090;"IP1750,2300,9250,7150;"
1670            OUTPUT @Hp7090;"IZ1750,2300,9250,7150;"
1680            OUTPUT @Hp7090;"GL10,10;"
```

```
1690            OUTPUT @Hp7090;"SP1,DG0;"
1700            OUTPUT @Hp7090;"PU;"
1701            LINPUT "DO YOU WANT LABELLING ?",Ans$
1702            IF Ans$="N" THEN 1920
1710            !
1720            !Label X and Y axis
1730            DISP "LABELLING"
1740            OUTPUT @Hp7090;"SI.2,.3;DI;"
1750            FOR X=0 TO 1000 STEP 100
1760                OUTPUT @Hp7090;"PA";X;",0;"
1770                READ A
1780                OUTPUT @Hp7090 USING "K";"CP0,-.5;LO5;LB";A;""
1790            NEXT X
1800            DATA -10,-8,-6,-4,-2,0,2,4,6,8,10
1810            OUTPUT @Hp7090;"PA500,-80;LBAngle(degrees)"
1820            FOR Y=0 TO 1000 STEP 200
1830                OUTPUT @Hp7090;"PA1.";Y;";"
1840                OUTPUT @Hp7090;"CP-.5,0;LO8;LB";Y/2000;""
1850            NEXT Y
1851            LINPUT "DO YOU WANT  DRAW NORMALIZATION ONLY ? ",Answer$
1852            IF Answer$="Y" THEN 1912
1860            OUTPUT @Hp7090;"SP1;PA-50,600;DI0,1;LT;"
1870            OUTPUT @Hp7090;"LO5;LBRaw data(volts) ---"
1880            OUTPUT @Hp7090;"SP2;PA-70,600;DI0,1;LT;"
1890            OUTPUT @Hp7090;"LO5;LBBeam intensity  ---"
1900          ! OUTPUT @Hp7090;"SP5;PA-90,600;DI0,1;LT;"
1910          ! OUTPUT @Hp7090;"LO5;LBNormalized intensity  ---"
1911            GOTO 1920
1912            OUTPUT @Hp7090;"SP5;PA-50,600;DI0,1;LT;"
1913            OUTPUT @Hp7090;"LO5;LBNormalized intensity   ---"
1920            RETURN
1930            !
1940            !
1950  END
```

LIST OF REFERENCES

1. **Saglam, Ahmet.**, *Cerenkov Radiation*, Master's Thesis, Naval Postgraduate School, Monterey, California, December 1982.

2. **Bruce, R. G.**, *Cerenkov Radiation From Periodic Bunches For A Finite Path In Air*, Master's Thesis, Naval Postgraduate School, Monterey, California, December 1985.

3. **O'Grady, A. J.**, *Cerenkov Radiation, Transition Radiation and Diffraction Transition Radiation from Periodic Bunches for a Finite Beam Path in Air*, Master's Thesis, Naval Postgraduate School, Montery, California, June 1986.

4. **Lee, Young–Moon.**, *Diffraction Transition Radiation from Periodic Electron Bunches*, Master's Thesis, Naval Postgraduate School, Monterey, California, December 1987.

5. **Jelley, J. V.**, *Cerenkov Radiation* and *Its Applications*, Pergamon Press, 1958.

6. **Ter–Mikaelian, M. L.**, *High–Energy Electromagnetic Processes In Condensed Media*, Wiley–Interscience, 1972

7. **Buskirk, F. R., and Neighbours, J. R.**, "Cerenkov Radiation from Periodic Electron Bunches", *Physical Review*, v. 28. pp. 1531–1535, September 1983.

8. Naval Postgraduate School Report Number NPS–61–83–010, *Diffraction Effects in Cerenkov Radiation*, by **F. R. Buskirk and J. R. Neighbours**, June 1983

9. Naval Surface Weapons Center Technical Report Number NSWC TR 84–134, *The Use of Transition Radiation As A Diagnostic For Intense Beams*, by **D. W. Rule and R. B. Fiorito**, July 1984.

10. **Ginsburg, V. L. and Frank, I. M.,** *Radiation of a Uniformly Moving Electron Due to its Transition from One Medium to Another*, Zhurnal Eksperimental'noi i Teoreticheskoi Fiziki, v 16, p. 15, 1946.

11. **Weast, R. C., and others,** *Handbook of Chemistry and Physics*, 69th ed., p. 495, CRC Press, March 1988.

INITIAL DISTRIBUTION LIST

		No. Copies
1.	Defense Technical Information Center Cameron Station Alexandria, Virginia 22304–6145	2
2.	Library, Code 0142 Naval Postgraduate School Monterey, California 93943–5002	2
3.	Department Chairman, Code 61 Department of Physics Naval Postgraduate School Monterey, California 93943–5004	1
4.	Prof. Xavier. K .Maruyama, Code 61Mx Department of Physics Naval Postgraduate School Monterey, California 93943–5004	2
5.	Prof. Fred R. Buskirk, Code 61Bs Department of Physics Naval Postgraduate School Monterey, California 93943–5004	2
6.	Wee, Kyoum Bok 500 Kwang–Ju Si, Buk–Gu, Jung–Heung Dong, 686–4 Seoul, Korea	2
7.	Yoon, Seog–Goo White Drive, C, #4 Tallahasse, Florida 32304	1
8.	Maj. Han, Hwang Jin SMC 2402 Naval Postgraduate School Monterey, California 93943–5000	1
9.	Maj. Kim, Jong Ryul SMC 1659 Naval Postgraduate School Monterey, California 93943–5000	1

10. Maj. Yoon, Duck Sang 1
SMC 1254
Naval Postgraduate School
Montery, California 93943–5000

11. Library 1
130–02
Korea Military Academy
Gong–Reung Dong, 556 -21
Seoul, Korea